Response to Reviewer Comments

January 19, 2019

Author Statement

We thank both referees for their time to review this manuscript as well as their constructive critiques and suggestions. Both referees write that the manuscript is suitable for publication in ACP. The two major suggestions were (1) to expand the introduction to include material that was only presented in the discussion (referee #1), and (2) to explicitly discuss the thermodynamically favored morphology (referee #2). The requested material has been added to the manuscript. Below are itemized responses explaining how all of the referees' critiques were addressed.

Response to Reviewer #1

Overview (Referee)

In the study at hand, Tandon and co-workers investigate the role of hydrophobic organic material on the cloud condensation ability of ammonium sulfate (AS) particles by coating them with polyethylene (PE). In this careful study with innovative design, no effect of the coatings was observed, rendering hydrophobic organic coatings as uninfluential under the investigated conditions. The paper is well-written, the topic is of high relevance to the Atmospheric Chemistry and Physics community and fits well within the scope of Atmospheric Chemistry and Physics. [...]. Hence, despite few, small issues, I find this work very publishable and an interesting data point for the relevance of organic coatings for cloud activation. I can recommend it for publication in ACP after minor revision.

Comments

[1]Regarding the title, I have two issues with the use of "internally mixed" here.

[1] Referee

1. This paper really rather looking at the effect of organic coatings on inorganic particles (admittedly, by creating an internally mixed particle) instead of the effect of organic coating on internally mixed particles.
2. While it is a set phrase in the aerosol community, it might paint the picture of hydrophobic substances being "mixed in" with inorganic substances.

There are not big issues, but the title threw me off slightly in the beginning and I wonder if this addition is needed.

[2]*We changed the title. In addition to the point raised by the referee, "internally mixed" should really be applied to a population of particles, while this paper discusses the potential role of morphology in single particles.*

[2] *Response*

[3]**(TITLE) The effect of hydrophobic glassy organic material on the cloud conden-**

[3] **Revision**

sation nuclei activity of ~~internally mixed~~ particles with different ~~particle~~ morphologies

[4]The biggest critique for the relevance of this work must be, as the author's state themselves in their discussion, the relevance of PE coatings for atmospheric particles. PE is indeed very different to the most common organic material in the atmosphere, Secondary Organic Material (SOM). The authors argue that SOM is rather irrelevant for this study since it is hydrophilic and hence would activate regardless under supersaturated conditions, but the authors have to do a better job communicating this early on in the article and providing proof. Since only a few corner cases can be thought of where a hydrophobic, viscous coating similar to PE might be generated in the atmosphere, it seems correct to at least describe the expected behavior of the vast majority of organic material that is present in the atmosphere. Here, it would be worthwhile to briefly summarize the effects of these glassy, but hydrophilic, coatings to water uptake under subsaturated conditions, a research topic that has received much attention in the past (Mikhailov et al., 2009, Zobrist et al., 2011, Berkemeier et al. 2014, Pajunoja et al., 2015, to name a few studies that looked at water uptake [kinetics]). The authors discuss this issue very openly in Sect. 4, however, this discussion is absent from the introduction.

[4] Referee

[5]*The introduction was revised as follows.*

[5] *Response*

[6]**(INTRODUCTION) Atmospheric aerosol sometimes consists of mixed particles with inorganic and organic components present in comparable mass fractions (Cruz and Pandis, 2000; Pöschl et al., 2010; Prenni et al., 2003). Most of the inorganic ~~particles~~compounds, commonly salts, are hygroscopic. The organic fraction is composed of a large number of compounds, many of which remain unspeciated. The contribution of the organic fraction to cloud condensation nuclei (CCN) activity depends on their hygroscopicity. The effective hygroscopicity parameter (Petters and Kreidenweis, 2007) of organic compounds varies between 0 and ~0.3, which is based on laboratory, field, and modeling studies (e.g. Prenni et al. 2007; Gunthe et al. 2009; Mikhailov et al., 2009; Chang et al. 2010; Massoli et al. 2010; Cappa et al. 2011; Mei et al. 2013; Pajunoja et al., 2015; Petters et al. 2016; Nakao 2017). ~~In contrast, a~~ A ~~number~~ small subset of species constituting the organic fraction, e.g. long chain n-alkanes with carbon number 16 and above and their fatty acids, have very low water affinity (Jacobson et al., 2000; Jimenez et al., 2009; Petters et al., 2016). The organic fraction can thus be divided into hydrophobic and hydrophilic compounds. Hydrophobic compounds do not take up water and do not contribute to CCN activity. Particles containing both organic and inorganic compounds may assume different phase states and morphologies.**

[6] **Revision**

The phase state of dry organic matter may be crystalline, amorphous solid or semisolid, or liquid. When formed from drying of aqueous solutions droplets,

the organic phase often partially or fully encapsulates the inorganic core (e.g. Ciobanu et al., 2009; Freedman et al., 2010; Reid et al., 2011; Krieger et al., 2012; Stewart et al., 2015; Altaf and Freedman, 2017). Bigg (1986) first suggested that organic compounds located at the particle surface may kinetically retard water uptake and thus reduce the particle's ability to promote CCN activity. This reduction in CCN activity may occur through several pathways. First, the mass accommodation coefficient of water may be reduced (e.g. Chuang et al., 1997; Nenes et al., 2001). Second, slow dissolution kinetics may reduce the number of dissolved molecules in the aqueous solution (Asa-Awuku and Nenes, 2007; O'Meara et al., 2016). Finally, high viscosity may slow diffusion of water (e.g. Zobrist et al., 2011) and thus may affect hygroscopic growth under subsaturated conditions (Mikhailov et al., 2009), especially at cold temperature (Berkemeier et al., 2014; Petters et al., 2019). Measurements of the diffusion coefficient of water through hydrophilic viscous matrices (Price et al., 2015), measurements of the equilibration time scale of glassy hydrophilic organic compounds with water at high RH (Rothfuss et al., 2018), and measurements of the interplay between viscosity, hygroscopic growth, and CCN activity (Pajunoja et al., 2015) suggest that hydrophilic liquid or hydrophilic amorphous solid organic matrices are unlikely to hinder droplet activation. The main reason for this behavior is that small amounts of water uptake plasticize the organic phase, which in turn removes diffusion limitations. Plasticization, however, does not occur in hydrophobic organic substances, which therefore are more plausible candidate compounds to kinetically limit water uptake and droplet activation.

Laboratory studies have tested the influence of hydrophobic organic coatings on hygroscopic growth and CCN activity (Abbatt et al., 2005; Cruz and Pandis, 1998; Garland et al., 2005; Hämeri et al., 1992; Nguyen et al., 2017; Ruehl and Wilson, 2014; Xiong et al., 1998). ...

The abstract reads especially strong: "it is concluded that mass transfer limitations by glassy organic shells are unlikely to affect cloud droplet activation near laboratory temperatures". As long as the authors do not show experiments with atmospherically more relevant material, this conclusion cannot stand by itself.

[7] *The conclusion is based on the synthesis of literature data (which was included in the original statement) and the data presented here. We weakened the statement from "concluded" to "suggested".*

[7] *Response*

[8] **Based on these results, and a synthesis of literature data, it is ~~concluded~~ suggested that mass transfer limitations by glassy organic shells are unlikely to affect cloud droplet activation near laboratory temperatures.**

[8] **Revision**

[9] (also, p.9, l.17 needs a reference)

[9] Referee

[10]*Corrected*

[10] *Response*

[11]The two principle mechanisms of the delay are poor mass accommodation and diffusional limitation through the organic matrix (e.g. Chuang et al., 1997, Nenes et al., 2001, Zobrist et al., 2011). Either effect also implies some influence of particle morphology on CCN activation

[11] **Revision**

[12]The authors describe their experimental and theoretical approach in detail. However, could the authors, in simple words, recite from their 2016 paper (Rothfuss and Petters, 2016) how they infer the slope of the viscosity vs temperature curve from a coalescence experiment, which to me seems to be more like a point measurement of viscosity?

[12] Referee

[13]*The observed viscosity range is shown by the gray circles in the right panels of Figure 2. The highlighted text was inserted to the manuscript to clarify the range in the methods section.*

[13] *Response*

[14]The shape factor is converted to viscosity, η via a lookup table of modified Frenkel sintering theory (Pokluda et al., 1997; Rothfuss and Petters, 2016). Conditioner residence time, monomer diameter, and surface tension assumed in the conversion are t = 5 s, D_{mono} = 50 nm, and σ = 0.034 J m^{-2} , respectively. The assumed surface tension is based on measured values for polyethylene melts (Dettre and Johnson, 1966; Owens and Wendt, 1969). The inferred viscosity is only weakly dependent on the assumed surface tension value (Marsh et al., 2018; Rothfuss and Petters, 2016). Particle shape factors vary between $1 \leq \xi \leq 4$, which map to a narrow range of viscosity between 10^{-5} Pa s and 3×10^{-6} Pa s for the selected conditioner residence time, monomer diameter, and surface tension. The inferred temperature dependent viscosity over this range is fitted to a modified Vogel-FulcherTammann (VFT) equation (Rothfuss and Petters, 2017).

[14] **Revision**

[15]The authors make a reasonable case that the PE/AS dimer particles should exhibit core-shell morphology (e.g. change in mobility diameter), but also point out that they have no exact proof for that. Since these doubts are communicated clearly, I can concur with their approach. The authors give an explanation why the activated fraction for the core-shell particles never reaches unity (Figs. 4 and 5), a curious observation since without the thermal conditioning step, the activated fraction seems to go a little higher (at least at 0.62 % water supersaturation, Fig. 4). While their explanation seems logical overall, can they exclude the possibility that some of these 10-20 % of particles are PE/AS particles and don't activate because they are the only ones having a "true" core-shell morphology (not cracked, not partially-engulfed)? In general, the fitted line shown here is somewhat misleading since it doesn't account for the fact that activation does not reach unity.

[15] Referee

[16]*As stated in the text, our conjecture is that a small fraction of decharged monomers transmits through the electrostatic filter, wherefore the distribution contains some fraction of pure PE particles that will not activate. This conjecture is based on extensive characterization of particle transmission through the system, which are the topic of a separate publication that is in preparation for submission to Aerosol Science and Technology (Rothfuss et al., in prep.). However, we did not quantify monomore decharging during the experiment reported here. To prove that some particles are fully coated and others are not, we would need to have a single particle composition measurement to show that the aerosol passed to the CCN instrument is indeed externally mixed. We therefore cannot categorically exclude the possibility that a small fraction has a "true" core-shell morphology that inhibited activation. In response we revised the paragraph to allow for this possibility.*

[16] *Response*

[17]**In some experiments, the activated fraction did not approach unity at high supersaturation. For experiments with disparate diameter of AS and PE, e.g. 50 nm AS and 120 nm PE, the dimer diameter will approach that of the larger monomer. Since a small fraction of decharged monomers also transmits (Rothfuss and Petters, 2016, Petters, 2018), the distribution may contain~~s~~ some fraction of pure PE particles that will not activate. Thus, the lack of 100% activation at high SS is likely an artifact and not due to particle morphology. However, it is also possible that those particles are composed of PE/AS and have assumed a core-shell morphology that is sufficient to hinder activation.**

[17] **Revision**

Response to Reviewer #2

Summary comments (Referee)

The study by Tandon et al. investigates whether an organic hydrophobic glassy coating influences the cloud condensation nuclei activity of ammonium sulfate particles. To do this, polyethylene particles and ammonium sulfate particles of opposite charge were separately produced and then coagulated. The morphology of the resulting charge neutral mixed particles was varied by heating. These experiments showed that coatings up to volume fractions of 97% did not change the critical supersaturation of 50 nm ammonium sulfate particles. Assuming that heating changes the mixed particle morphology from partially to completely engulfed, the authors conclude that mass transfer limitations by glassy organic shells are unlikely to affect cloud droplet activation near laboratory temperatures. The authors address here a relevant and timely topic of atmospheric research that is well suited for publication in ACP. The experiments are intelligently designed and well performed.

Major Comment

[18]However, I have a major concern regarding the interpretation of the results that needs to be addressed before publication. Namely, the authors are too confident that the morphology is core-shell. Whether core-shell or partially engulfed morphologies are adopted depends on the surface tensions of the two involved phases and the interfacial tension between them. Estimating the spreading coefficient allows to predict which of these two morphologies is thermodynamically favored (Krieger et al., 2012; Reid et al., 2011). Partially engulfed configurations can also appear almost spherical and be misinterpreted as core-shell. Therefore, the spreading coefficient for the polyethylene-ammonium sulfate system should be calculated to assess the most likely morphology. Core-shell morphologies prevail in liquid-liquid-phase separated systems consisting of an aqueous organic and an aqueous inorganic phase (e.g. Ciobanu et al., 2009; Song et al., 2012; Stewart et al., 2015), while partially engulfed morphologies were observed for mixtures of hydrocarbons with NaCl, systems that come close to the one investigated in the present study. The authors showed that a hydrophobic coating does not impede CCN activation, however, most probably not because of lack of mass transfer limitations by glassy shells but due to an incomplete coating given by a partially engulfed morphology. This point needs to be adequately addressed before publication. The authors should reconsider their interpretation. They need to explain why their system should not relax into the thermodynamic favored state of partially engulfed.

[18] Referee

[19]*We thank the referee to push us to clarify what is and is not known about the formed particle morphology. Furthermore, it is true that partially engulfed particles may appear almost spherical and our technique is not yet sensitive enough to detect small differences in particle shape. This will be acknowledged in the revised text.*

The theory and experimental observations cited by the referee are not directly relevant to the system here. The spreading coefficient model discussed in Reid et al. (2011) and Krieger et al. (2012) goes back to Torza and Mason (1970) and describes two immiscible liquid

[19] *Response*

drops suspended in a third immiscible liquid. Similarly, the cited observations refer to the equilibrium morphology of liquid-liquid phase separated systems on supermicron droplets.

The case here is different. At high temperature a liquid polyethlyene droplet is in contact with a solid 50 nm diameter ammonium sulfate core. The assumed morphology of a sessile droplet on a spherical solid substrate depends on the solid/liquid, solid/vapor, liquid/vapor tensions, as well as the tension of the three phase contact line (Iwamatsu, 2016). The line tension term gains importance with decreasing particle diameter. Iwamatsu (2016) provides theory to predict the equilibrium morphology of such a system, which can be (1) complete wetting (core-shell morphology), (2) cap shaped droplet (core-shell spherical morphology with uneven coating thickness), (3) cap shaped droplet (partially engulfed morphology), (4) complete drying (dumbbell shaped morphology).

We do not know all relevant tensions to predict the shape. We know the liquid/vapor tension of polyethlene melts (0.034 J m-2, Dettre and Johnson, 1966; Owens and Wendt, 1969) and we expect that the solid/vapor tension of ammonium sulfate exceeds 0.080 J m-2, the value of concentrated solutions with water (Petters and Petters, 2016). The latter assumption is based on the notion that the saturated solution can approximate the surface tension of the solid/vapor interface and the analogous solid/vapor interface for NaCl, where the solid/vapor tension slightly exceeds that of the liquid/vapor tension of the saturated solution (Bahadur et al., 2007). We do not know the liquid/solid tension, the line tension or Young's contact angle of liquid PE on ammonium sulfate. Thus a theoretical prediction is not possible. However, we offer some discussion that argues in favor of complete wetting, i.e. core-shell morphology.

1. *Assuming that line tension is neglible, Young's law applies*

   $$\gamma_{sg} - \gamma_{sl} = \gamma_{lg} \cos\theta_Y$$

   where $\gamma_{sg}, \gamma_{sl}, \gamma_{lg}$ *are the solid/gas, solid/liquid, and liquid/gas interfacial tensions and* θ_Y *is Young's contact angle. Wetting occurs as* θ_Y *approaches* 0°*. Given that* γ_{sg} *of inorganic salts is large (here estimated* $>$ *0.08 J m-2) and* γ_{lg} *is small for liquid PE (*$<$ *0.034 J m-2), wetting will occur even if* γ_{sl} *were appreciable (*$<$ *0.046 J m-2). (A large* γ_{sl} *implies repulsive forces between the substrate and the liquid). In general, a low liquid/vapor surface tension will favor wetting and the liquid/gas tension term often dominates.*

2. *Wetting at nanonscale is more efficient than at microscale. The stability diagram given by Iwamatsu (2016, their Fig. 7) suggests that for a sessile droplet on a spherical solid substrate wetting even occurs for* $\theta_Y > 0^\circ$*. The upper contact angle where complete wetting is observed varies. This implies that even stronger respulsive forces than implied in* γ_{sl} *= 0.046 J m-2 could be overcome in nanoscale systems due to the line tension effect.*

3. *In the absence of theoretical predictions, findings from the literature are presented to corroborate the conjecture that complete wetting by liquid PE is plausible.*

   (a) *Freedman et al. (2010) show that ammonium sulfate particles coated with palmitic acid (produced through a coating oven), remain in core-shell structure. Palmitic acid and liquid PE both have low liquid/vapor interfacial tension. Palmitic acid and PE* *are both dominated by CH2 groups and thus* γ_{sl} *for these two substances should be similar.*

(b) *Reid et al. (2011) argue that the assumption that core–shell morphologies are formed "is well founded for a liquid phase surrounding a solid crystalline core". The effect cited by the referee that partially engulfed morphologies are observed for mixtures of hydrocarbons with aqueous NaCl is, to our understanding, due to the lowering of the aqueous solution surface tension by the organic, which does not occur in the crystalline case.*

Despite the above, we freely acknowledge that (1) near spherical particle shape does not preclude partially engulfed morphology, (2) that we do not have emprical proof of particle morphology, (3) that the possibility of partially engulfed morphology cannot be easily dismissed, and (4) that forces during annealing may alter the equilibrium morphology of the liquid PE/solid AS particle. We have added a paragraph that discusses the possible morphologies, and include partially engulfed equilibrium morphology in the list of possible explanations why not kinetic limitations were observed.

[20] **Revision**

[20]**Since the melting point of AS (280 °C, Lide and Haynes, 2009) is much higher than that of PE (107 °C) the liquid PE is expected to partially or fully engulf the AS core. The assumed morphology of a liquid droplet on a spherical solid substrate depends on the solid/liquid, solid/vapor, liquid/vapor tensions, as well as the tension of the three phase contact line (Iwamatsu, 2016). The equilibrium morphology of this system can be (1) core-shell morphology (complete wetting), (2) core-shell morphology with uneven coating thickness (cap shaped droplet), (3) partially engulfed morphology (cap shaped droplet), or (4) dumbbell shaped morphology (complete drying). Parenthetical terms correspond to those used by Iwamatsu (2016). The line tension term becomes increasingly important at smaller scales. Line tension drives the system toward core-shell morphology. There is insufficient information about the AS/PE system at 95 °C to theoretically evaluate the equilibrium morphology. However, the liquid/vapor tension of polyethylene melts is 0.034 J m-2 (Dettre and Johnson, 1966; Owens and Wendt, 1969) and in principle a low liquid/vapor tension will favor the spreading of liquid on a high-energy surface. Reid et al. (2011) argue that core–shell morphologies are favored for a liquid phase surrounding a solid crystalline core. Freedman et al. (2010) show that ammonium sulfate particles coated with palmitic acid (produced through a coating oven), remain in core-shell structure. Palmitic acid and liquid PE both have low liquid/vapor interfacial tension. Palmitic acid and PE are both dominated by CH2 functional groups and thus the solid/liquid tension and line tension terms for these two substances should be similar.**

The particles are cooled down to system temperature after they relax into spherical shape in the temperature-controlled loop. Based on the above we argue that the final morphology is a core-shell structure. However, we cannot dismiss the possibility that particles assumed a partially engulfed morphology. That morphology may be either due to equilibrium shape or arise during the anneal-

ing of the particle. ~~Upon cooling the PE coating anneals.~~ Thus, w~~W~~hether the coating of annealed PE is of uniform thickness is unknown. Scanning Electron Microscopy with Energy Dispersive X-ray spectroscopy of PE/AS dimer particles with larger diameters was attempted. However, the analysis was inconclusive due to insufficient resolution resulting from poor conductivity of the prepared samples and necessary limits in maximum electron beam intensity to ensure that the PE did not melt.

Specific Comments

[21]Page 1, line 14: polyethylene is taken as proxy for hydrophobic glass organic material. PE has a C:O ratio of zero. This is too low for a good proxy of atmospheric hydrophobic material.

[21] Referee

[22]*This has been addressed in response to comment [37]Referee (see below).*

[22] *Response*

[23]The expression “dimers” is used to refer to mixed polyethylene-ammonium sulfate particles. The definition of ”dimer” in the online Oxford dictionary is: “A molecule or molecular complex consisting of two identical molecules linked together.” The Collins English Dictionary defines: “a molecule composed of two identical simpler molecules (monomers).” In the present study, “dimer” is used for particles obtained by coalescing two chemically very diverse particles. The authors should refrain from using “monomers” and “dimers” and search for alternative expressions.

[23] Referee

[24]*The usage of monomer and dimer in the context of our method has not yet been critiqued by any of the referees of five prior publications. Google search results for “monomer particle” and “dimer particle” show 7760 and 2200 results, which appear predominately from the scientific literature, including the aerosol literature. We believe that meaning of the terms monomer and dimer in the manuscript is clear. Nonetheless, we have also added the clarifying particle to the abstract and include a strict definition in the text.*

[24] *Response*

[25]**(ABSTRACT) ... charge-neutral polyethylene-ammonium sulfate dimer~~s~~ particles were then isolated for online observation. Morphology of these dimer~~s~~ particles was varied by heating, such that liquefied polyethylene partially or completely engulfed the ammonium sulfate.**

[25] **Revision**

(INTRODUCTION) ... is used to generate mixed particles composed of PE/PE and PE/AS dimer particles. Viscosity and CCN activity of pure PE particles is quantified. Dimer particle morphology

(METHODS) The basic methodology for dimer particle preparation has been presented in detail elsewhere (Marsh et al., 2018; Rothfuss and Petters, 2016). Briefly, two monodisperse particle populations of opposite charge are generated using differential mobility analyzers (DMAs) operated with positive and negative polarity power supplies. The streams are merged and particles are given time to coagulate. Coagulated dimer~~s~~ particles from particles carrying +1/–1 charge are charge neutral and transmit through an electrostatic filter. The terms “monomer particle” or monomer are used to refer to particles transmitted by a single DMA and the term “dimer particle” or dimer are used to refer coagulated particles. These particles are available for further manipulation and measurement.

[26]Page 4, line 7 - 13: how was the morphology determined? Partially engulfed particles might appear almost spherical and still, the engulfed phase is in contact with the gas phase.

[26] Referee

[27]*Morphology is only determined indirectly via change in drag force. It is therefore correct that partially engulfed might appear almost spherical and this is included in the revision. (Please see response to the major comment.)*

[27] *Response*

[28]Page 7, lines 24 – 32: Here it is explicitly stated that the exact morphology could not be determined experimentally. Therefore, the authors should infer it from thermodynamic considerations using the spreading coefficient.

[28] Referee

[29]*Please see response to major comment.*

[29] *Response*

[30]Page 8, lines 24: “core/shell” should be replaced by “spherical”.

[30] Referee

[31]*Please see response to major comment.*

[31] *Response*

[32]Page 10, lines 1 – 13: long chain fatty acids are a completely different case than PE, because they are surface active and should therefore fully cover the AS surface. Therefore, fatty acid coatings can very well hinder water transfer while a PE coating does not.

[32] Referee

[33]*Please see our response to major comment.*

[33] *Response*

[34]Page 10, line 19 – 20: Do you have any indication that the carbon number may have changed?

[34] Referee

[35]*We do not but thermal decomposition of polymers is a possibility that deserves to be*

[35] *Response*

mentioned. We revised as follows.

[36]**The carbon number may have changed during heating via thermal decomposition ~~during particle generation~~. Whether or not this occurred cannot be determined from the available data. Regardless, the obtained PE particles had an estimated viscosity of 10^{12} Pa s at room temperature.** [36] **Revision**

[37]Page 10, lines 17 – 19: As stated above PE is not a good surrogate for high molecular weight weakly functionalized hydrocarbons: atmospherically relevant hydrophobic organics usually carry more double bonds and more aromatic rings. Moreover, the O:C ratio is zero for PE, which is hardly found in ambient organic aerosols. [37] Referee

[38]*We added this caveat.* [38] *Response*

[39]**The exact carbon number of the PE particles here is not important, addition or subtraction of a few CH2 molecules does not significantly alter viscosity or hygroscopity (Petters et al., 2016; Rothfuss and Petters, 2017). Note, however, that atmospherically relevant hydrophobic organics may have double bonds, include aromatic rings (e.g. polycyclic aromatic hydrocarbons), and may include some functional groups other than CH_x. ~~.~~Nonetheless, ~~T~~the PE particles used here are ~~therefore~~ used as a proxy for hydrophobic and glassy compounds.** [39] **Revision**

[40]Page 10, lines 29 – 31: It is not necessary to invoke fissures because the surface tension forces will NOT lead to a completely engulfed core with uniform coating. See my general comment. [40] Referee

[41]*Please see response to general comment.* [41] *Response*

[42]Page 11. Lines 10 – 29: These conclusions need to be rewritten: With the experiments performed with PE, water transfer limitations and a low mass accommodation coefficient cannot be ruled out in the case of fatty acid coatings. If a hydrophobic organic mixture contains a share of surface active species, it might very well hinder CCN activation. The type of experiment performed in this study needs to be repeated with fatty acid containing hydrocarbons to come to a conclusion. [42] Referee

[43]*CCN experiments with hydrophobic organic materials of low viscosity, including saturated and unsaturated fatty acids have been performed extensively in the literature (Cruz and Pandis 1998; Abbatt et al., 2005; Nguyen et al., 2017; Forestieri et al., 2018). These are discussed in the introduction and show with the exception of thickly coated palmitic acid that no hindrance in CCN activation was observed. Even the most favorable case, NaCl with > 60% palmitic acid (the referees hydrophobic surface active organic), changed the net* [43] *Response*

kappa only slightly. There are only two out of many data points in Nguyen et al. (2017, their Fig. 6) that show this behavior, and it is not entirely clear how measurement errors and uncertainties about the assumptions in the calculation (e.g. change in particle shape, evaluation of coating thickness) would factor into their closure calculation between predicted and observed kappa. Nguyen et al. (2017) write

> *"For the saturated palmitic acid, a slight negative deviation (smaller observed kappa value than predicted) from the kappa addition rule was observed at thick coatings. It seems likely that this is due to limited diffusion of water through a solid coating as discussed above."*

We don't disagree with that statement. However, the overwhelming number of data points in Nguyen et al. (2017) and all data from the remaining studies show no effect of fatty acid coatings on CCN activity. Given that the fatty acid/NaCl system has been extensively studied, we disagree with the referee that we need to repeat these experiments to factor it into a conclusion.

As to the broader point, the paragraph in question essentially argues that it is almost impossible to demonstrate kinetic limitations of in the lab. It is difficult to imagine processes that lead to more effective coatings in the atmosphere when compared to the laboratoru. We still believe that this conclusion is justified. However, the statement was revised to include partially engulfed morphologies and weakened the conclusion to the "majority of cases".

[44]**Regardless, the imagined processes producing hydrophobic glassy coatings undergo drying and cooling cycles that will be susceptible to the same ~~three~~ issues reported here: cracks, ~~and~~ non-uniform coating thickness formed during drying or annealing, partially engulfed equilibrium morphology~~,~~ and faster than expected diffusion through hydrocarbon films. We therefore conclude that mass transfer limitation by glassy organic shells is unlikely to affect cloud droplet activation in the majority of cases at temperatures prevalent in the lower atmosphere. Extension of this result to temperatures in the upper free troposphere where low temperature slows diffusion may require further experimentation.**

[44] **Revision**

[45]Page 12, lines 23 – 25: "Potential explanations are cracks formed during annealing, non-uniform coating thickness, or fast diffusion of small molecules through polymer membranes. It is argued that processes that may form glassy hydrophobic organic shells on atmospheric particles will result in similar imperfect shielding of hygroscopic cores." The explanation is a partially engulfed morphology. As stated above, this explanation might not hold for a fatty acid coatings. Therefore, this conclusion is not valid and needs to be removed.

[45] Referee

[46]*Please see our response to the major comment regarding partially engulfed morphology. It is stated in the introduction that the evidence is scant that fatty acid coatings hinder activation. However, we agree that it worthwhile adding a qualifying statement that thickly coated stearic acid may lead to hindrance.*

[46] *Response*

[47]**Potential explanations are cracks formed during annealing, non-uniform coat-**

[47] **Revision**

ing thickness, formation of partially engulfed morphologies, or fast diffusion of small molecules through polymer membranes. It is argued that processes that may form glassy hydrophobic organic shells on atmospheric particles will result in similar imperfect shielding of hygroscopic cores. However, particles with thick coatings of some, but not all fatty acids are an exception to the preceding claim (Abbatt et al., 2005, Nguyen et al., 2017, Forestieri et al., 2018).

[48]Page 21, figure caption of Fig. 2: what is the definition of the "mean shape factor"? It has not been defined in the main text. Is it the same as the "geometry factor"?

[48] Referee

[49]*Corrected.*

[49] *Response*

[50]**(METHODS) Next, the fitted mode diameters are binned into 3 K intervals (Marsh et al., 2018) and the mean geometry factor is derived for each bin. These data are then fitted to a logistic curve** [51]**Figure 2. Left plots: shape relaxation data for PE/AS (a) and PE/PE (c) 50nm/50nm dimers. Symbols are the mean ~~shape~~geometry factor derived from the temperature binned mode diameter peaks.**

[50] **Revision**

[51] **Revision**

[52]Page 21, figure caption of Fig. 2: what is the definition of "viscosity temperature"? Again, this has not been defined in the main text?

[52] Referee

[53]*This was poor wording.*

[53] *Response*

[54]**Right plots: ~~inferred viscosity~~ temperature dependence of viscosity for PE/AS (b) and PE/PE (d) experiments.**

[54] **Revision**

[55]Technical corrections: Page 2, line 4: maybe better: "small gas molecules" instead of small gases Page 5, line 14: "where" instead of "were" Page 8, line 7: "charged" instead of "charge".

[55] Referee

[56]*Corrected.*

[56] *Response*

References Cited

Highlighted references were added to the manuscript. Non-highlighted references are used in response to referees. References that appeared in the original manuscript are cited there.

Bahadur, R. Russell, L. M., Alavi, S.: Surface Tensions in NaCl-Water-Air Systems from MD Simulations, J. Phys. Chem. B, 111, 11989–11996, 2007.

Berkemeier, T., Shiraiwa, M., Pöschl, U., and Koop, T.: Competition between water uptake and ice nucleation by glassy organic aerosol particles, Atmos. Chem. Phys., 14, 12513-12531, https://doi.org/10.5194/acp-14-12513-2014, 2014.

Cappa, C. D., Che, D. L., Kessler, S. H., Kroll, J. H. and Wilson, K. R.: Variations in organic aerosol optical and hygroscopic properties upon heterogeneous OH oxidation. Journal of Geophysical Research: Atmospheres, 116, D15204, 2011.

Chang, R. Y.-W., Slowik, J. G., Shantz, N. C., Vlasenko, A., Liggio, J., Sjostedt, S. J., Leaitch, W. R., and Abbatt, J. P. D.: The hygroscopicity parameter (κ) of ambient organic aerosol at a field site subject to biogenic and anthropogenic influences: relationship to degree of aerosol oxidation, Atmos. Chem. Phys., 10, 5047-5064, https://doi.org/10.5194/acp-10-5047-2010, 2010.

Chuang, P. Y., Charlson, R. J. and Seinfeld, J. H.: Kinetic limitations on droplet formation in clouds, Nature, 390, 594, 1997.

Ciobanu, V. G., Marcolli, C., Krieger, U. K., Weers, U. and Peter, T.: Liquid-liquid phase separation in Mixed Organic/Inorganic Aerosol Particles, J. Phys. Chem. A, 113, 10966–10978, doi:10.1021/Jp905054d, 2009.

Freedman, M. A., Baustian, K. J., Wise, M. E. and Tolbert, M. A.: Characterizing the Morphology of Organic Aerosols at Ambient Temperature and Pressure, Analytical Chemistry, 82(19), 7965–7972, 2010.

Gunthe, S. S., King, S. M., Rose, D., Chen, Q., Roldin, P., Farmer, D. K., Jimenez, J. L., Artaxo, P., Andreae, M. O., Martin, S. T., and Pöschl, U.: Cloud condensation nuclei in pristine tropical rainforest air of Amazonia: size-resolved measurements and modeling of atmospheric aerosol composition and CCN activity, Atmos. Chem. Phys., 9, 7551-7575, https://doi.org/10.5194/acp-9-7551-2009, 2009.

Iwamatsu, M.: Line tension and morphology of a sessile droplet on a spherical substrate, Phys. Rev. E, 93, 052804, 2016.

Krieger, U. K., Marcolli, C., Reid, J. P.: Exploring the Complexity of Aerosol Particle Properties and Processes using Single Particle Techniques, Chem. Soc. Rev., 41, 6631–6662, 2012.

Massoli, P., Lambe, A. T., Ahern, A. T., Williams, L. R., Ehn, M., Mikkilä, J., Canagaratna, M. R., Brune, W. H., Onasch, T. B., Jayne, J. T., Petäjä, T., Kulmala, M., Laaksonen, A., Kolb, C. E., Davidovits, P., and Worsnop, D. R.: Relationship between aerosol oxidation level and hygroscopic properties of laboratory generated secondary organic aerosol (SOA) particles, Geophys. Res. Lett., 37, L24801, https://doi.org/10.1029/2010GL045258, 2010.

Nakao, S.: Why would apparent κ linearly change with O/C? Assessing the role of volatility, solubility, and surface activity of organic aerosols. Aerosol Sci. Technol., 51, 1377-1388, 2017.

Mei, F., Setyan, A., Zhang, Q., and Wang, J.: CCN activity of organic aerosols observed downwind of urban emissions during CARES, Atmos. Chem. Phys., 13, 12155-12169, https://doi.org/10.5194/acp-13-12155-2013, 2013.

Nenes, A., Ghan, S., Abdul-Razzak, H., Chuang, P. Y. and Seinfeld, J. H.: Kinetic limitations on cloud droplet formation and impact on cloud albedo, Tellus B, 53(2), 133-149, 2001.

O'Meara, S., Topping, D. O., and McFiggans, G.: The rate of equilibration of viscous aerosol particles, Atmos. Chem. Phys., 16, 5299-5313, https://doi.org/10.5194/acp-16-5299-2016, 2016.

Pajunoja, A., Lambe, A. T., Hakala, J., Rastak, N., Cummings, M. J., Brogan, J. F., Hao, L., Paramonov, M., Hong, J., Prisle, N. L., Malila, J., Romakkaniemi, S., Lehtinen, K. E. J., Laaksonen, A., Kulmala, M., Massoli, P., Onasch, T. B., Donahue, N. M., Riipinen, I., Davidovits, P., Worsnop, D. R., Petäjä, T., and Virtanen, A.: Adsorptive uptake of water by semisolid secondary organic aerosols, Geophys. Res. Lett., 42, 3063–3068,https://doi.org/10.1002/2015GL063142, 2015.

Petters, S. S., Kreidenweis, S. M., Grieshop, A. P., Ziemann, P. J., & Petters, M. D.: Temperature- and humidity-dependent phase states of secondary organic aerosols, Geophys. Res. Lett., 46, https://doi.org/10.1029/2018GL080563, 2019.

Prenni, A. J., Petters, M. D., Kreidenweis, S. M., DeMott, P. J. and Ziemann, P. J.: Cloud droplet activation of secondary organic aerosol, J. Geophys. Res.,112, D10223, doi:10.1029/2006JD007963, 2007.

Reid, J. P., Dennis-Smither, B. J., Kwamena, N.-O. A., Miles, R. E. H., Hanford, K. L. and Homer, C. J.: The morphology of aerosol particles consisting of hydrophobic and hydrophilic phases: hydrocarbons, alcohols and fatty acids as the hydrophobic component, Phys. Chem. Chem. Phys., 13(34), 15559–15572, 2011.

Stewart, D. J., Cai, C., Nayler, J., Preston, T. C., Reid, J. P., Krieger, U. K., Marcolli, C. and Zhang, Y. H.: Liquid–Liquid Phase Separation in Mixed Organic/Inorganic Single Aqueous Aerosol Droplets, J. Phys. Chemistry A, 119(18), 4177–4190, 2015.

Torza, S. and Mason, S. G.: Three-Phase Interactions In Shear and Electrical Fields, Journal of Colloid and Interface Science, 33(1), 67–83,1970.

Zobrist, B., Soonsin, V., Luo, B. P., Krieger, U. K., Marcolli, C., Peter, T. and Koop, T.: Ultra-slow water diffusion in aqueous sucrose glasses, Phys. Chem. Chem. Phys., 13(8), 3514–3526, 2011.

The effect of hydrophobic glassy organic material on the cloud condensation nuclei activity of ~~internally mixed~~ particles with different ~~particle~~ morphologies

Ankit Tandon[1, 2], Nicholas E. Rothfuss[1], Markus D. Petters[1]

[1]Department of Marine Earth and Atmospheric Sciences, North Carolina State University, Raleigh, 27695-8208, USA
[2]School of Earth and Environmental Sciences, Central University of Himachal Pradesh, Dharamshala, 176215, India

Correspondence to: Markus D. Petters (markus_petters@ncsu.edu)

Abstract. Particles composed of organic and inorganic components can assume core-shell morphologies. The kinetic limitation of water uptake due to the presence of a hydrophobic viscous outer shell may increase the critical supersaturation required to activate such particles into cloud droplets. Here we test this hypothesis through laboratory experiments. Results show that the viscosity of polyethylene particles is 5×10^6 Pa s at 60 °C. Extrapolation of temperature dependent viscosity measurements suggests that the particles are glassy at room temperature. Cloud condensation nuclei (CCN) activity measurements demonstrate that pure polyethylene particles are CCN inactive at diameters less than 741 nm and 2.5% water supersaturation. Thus, polyethylene is used as proxy for hydrophobic glassy organic material. Ammonium sulfate is used as proxy for hygroscopic CCN active inorganic material. Mixed particles were generated using coagulation of oppositely charged particles; charge-neutral polyethylene-ammonium sulfate dimer~~s~~ particles were then isolated for online observation. Morphology of these dimer~~s~~ particles was varied by heating, such that liquefied polyethylene partially or completely engulfed the ammonium sulfate. Critical supersaturation was measured as a function of dry particle volume, particle morphology, and organic volume fraction. The data show that kinetic limitations do not change the critical supersaturation of 50 nm ammonium sulfate cores coated with polyethylene and polyethylene volume fractions up to 97%. Based on these results, and a synthesis of literature data, it is ~~concluded~~ suggested that mass transfer limitations by glassy organic shells are unlikely to affect cloud droplet activation near laboratory temperatures.

1 Introduction

Atmospheric aerosol sometimes consists of mixed particles with inorganic and organic components present in comparable mass fractions (Cruz and Pandis, 2000; Pöschl et al., 2010; Prenni et al., 2003). Most of the inorganic ~~particles~~compounds, commonly salts, are hygroscopic. The organic fraction is composed of a large number of compounds, many of which remain unspeciated. The contribution of the organic fraction to cloud condensation nuclei (CCN) activity depends on their hygroscopicity. The effective hygroscopicity parameter (Petters and Kreidenweis, 2007) of organic compounds varies between 0 and ~0.3, which is based on laboratory, field, and modeling studies (e.g. Prenni et al. 2007; Gunthe et al. 2009; Mikhailov et al., 2009; Chang et al. 2010; Massoli et al. 2010; Cappa et al. 2011; Mei et al. 2013; Pajunoja et al., 2015; Petters et al. 2016; Nakao 2017). ~~In contrast, a~~ A ~~number~~ small subset of species constituting the organic fraction, e.g. long chain n-alkanes with carbon nu~~m~~ber 16 and above and their fatty acids, have very low water affinity (Jacobson et al., 2000; Jimenez et al., 2009; Petters et al., 2016). The organic fraction can thus be divided into hydrophobic and hydrophilic compounds. Hydrophobic compounds do not take up water and do not contribute to CCN activity.

Particles containing both organic and inorganic compounds may assume different phase states and morphologies. The phase state of dry organic matter may be crystalline, amorphous solid or semisolid, or liquid. When formed from drying of aqueous solutions droplets, the organic phase often partially or fully encapsulates the inorganic core (e.g. Ciobanu et al., 2009; Freedman et al., 2010; Reid et al., 2011; Krieger et al., 2012; Stewart et al., 2015; Altaf and Freedman, 2017). Bigg (1986) first suggested that organic compounds located at the particle surface may kinetically retard water uptake and thus reduce the particle's ability to promote CCN activity. This reduction in CCN activity may occur through several pathways. First, the mass accommodation coefficient of water may be reduced (e.g. Chuang et al., 1997; Nenes et al., 2001). Second, slow dissolution kinetics may reduce the number of dissolved molecules in the aqueous solution (Asa-Awuku and Nenes, 2007; O'Meara et al., 2016). Finally, high viscosity may slow diffusion of water (e.g. Zobrist et al., 2011) and thus affect hygroscopic growth under subsaturated conditions (Mikhailov et al., 2009), especially at cold temperature (Berkemeier et al., 2014; Petters et al., 2019). Measurements of the diffusion coefficient of water through hydrophilic viscous matrices (Price et al., 2015), measurements of the equilibration time scale of glassy hydrophilic organic compounds with water at high RH (Rothfuss et al., 2018), and measurements of the interplay between viscosity, hygroscopic growth, and CCN activity (Pajunoja et al., 2015) suggest that hydrophilic liquid or hydrophilic amorphous solid organic matrices are unlikely to hinder droplet activation. The main reason for this behavior is that small amounts of water uptake plasticize the organic phase, which in turn removes diffusion2 limitations. Plasticization, however, does not occur in hydrophobic organic substances, which therefore are more plausible candidate compounds to kinetically limit water uptake and droplet activation.

Laboratory studies have tested the influence of hydrophobic organic coatings on hygroscopic growth and CCN activity (Abbatt et al., 2005; Cruz and Pandis, 1998; Garland et al., 2005; Hämeri et al., 1992; Nguyen et al., 2017; Ruehl and Wilson, 2014; Xiong et al., 1998). Sometimes, but not always, a hydrophobic organic layer kinetically limits water up-take by the inorganic core and retards hygroscopic growth or CCN activity (Abbatt et al., 2005; Nguyen et al., 2017; Ruehl and Wilson, 2014; Xiong et al., 1998). These studies are now briefly reviewed. Significant work has been performed on characterizing the transfer of small gas~~e~~ molecules between an aqueous phase and the vapor phase separated by an organic film (McNeill et al., 2013). The review here is limited to transfer of water vapor. Studies summarizing results for N_2O_5, HCl, HNO_3 and other small molecules are reviewed elsewhere (McNeill et al., 2013).

Studies at subsaturated RH have been performed by several investigators. Hämeri et al. (1992) show that coatings of tetracosane (solid alkane), octanoic acid (liquid carboxylic acid), or lauric acid (solid carboxylic acid) do not prevent NaCl particles from deliquescing. Garland et al. (2005) reported that the deliquescence relative humidity for ammonium sulfate (AS) particles coated with palmitic acid was the same as for pure AS for particles with low organic mass fraction (~20%). For particles with higher mass fraction (~50%) of palmitic acid, full deliquescence required higher relative humidity. Xiong et al. (1998) experimentally examined the effects of organic films on the kinetic growth rate of ultrafine sulfuric acid aerosols in relation to film thickness and particle diameter. They reported that the monolayer films of lauric and stearic acid retard the hygroscopic growth rate of sulfuric acid aerosols. This reduction in hygroscopic growth was 20% for a 6 monolayer (14.4 nm) thick coating of lauric acid on 40-120 nm particles and relative humidity (RH) up to 85%. The slopes of hygroscopic growth factor-RH curves decrease significantly with increasing number of monolayers and residence time. However, for films ≥14.4 nm, the growth factor-RH curve remains the same regardless of coating thickness. Ruehl and Wilson (2014) measured the droplet size formed at 99.9% RH on submicrometer particles. Ammonium sulfate particles coated with palmitic and stearic acid did not take up water as expected suggesting an accommodation coefficient of 10^{-4}. Forestieri et al. (2018) report similar observations for NaCl particles coated with palmitic acid. Particles exceeding 80% organic fraction had reduced humidified droplet size at 99.88% RH, which was attributed to kinetic limitations. Gorkowski et al. (2017) created core-shell structures with secondary organic materials comprising the shell and found no diffusion limitations for water (and other substances) at humid conditions.

Studies examining the effect of organic coatings on CCN activation also show mixed results. Cruz and Pandis (1998) investigated the effect of organic coatings on the CCN activation of AS particles coated with glutaric acid or dioctylphthalate (DOP). The CCN activation behavior of a particle having an inorganic core with organic coating was predicted by Köhler theory and applying the Zdanovskii, Stokes, and Robinson (ZSR) assumption that the equilibrium water content of the mixed particle is additive. Particles with coatings of DOP constituting at least 70% mass of the mixed particle did not hinder activation. In contrast, Abbatt et al. (2005) observed a complete deactivation of AS particles that were thickly coated (> 13 nm) with stearic acid, although thinner coatings and other substances had no effect. Nguyen et al. (2017) reported that NaCl particles coated with palmitic and stearic acid lead to deviations from the ZSR rule consistent with kinetic limitations to water uptake. Unsaturated acids did not show any deviation from the ZSR rule. Forestieri et al. (2018) investigated the CCN activity of NaCl particles coated with oleic acid and mixtures of myristic acid/oleic acid and palmitic/oleic acid and found no deviation from the ZSR rule that would be indicative of kinetic limitations.

The most commonly used materials applied in coating studies are n-alkanes and fatty acids. These compounds are hydrophobic and CCN inactive (Petters et al., 2016). The phase state of these molecules is assumed to be either liquid or solid based on the bulk phase of the substance at room temperature. In most studies the proposed mechanism responsible for the hypothesized kinetic limitation has been a reduced mass accommodation coefficient, which hinders the kinetic rate of droplet growth. The mass accommodation coefficient is defined as the fraction of molecules that stick to the particle upon collision with the droplet. Related are kinetic limitation due to diffusional transfer through the organic material, which is controlled by the viscosity of the coating. Viscosity ranges from 10^{-3} Pa s for liquids to > 10^{12} Pa s for glassy substances (Reid et al., 2018). According to the Stokes-Einstein relationship the characteristic time required for water molecule to diffuse through a 10 nm thick coating is 69 s, 6.9×10^4 s, and 6.9×10^7 s for viscosity of 10^6, 10^9 and 10^{12} Pa s, respectively. Although it is known that the Stokes-Einstein relationship may not hold for water and high viscosity (Chenyakin et al., 2017; Price et al., 2014), increased viscosity still slows diffusion.

The above cited studies did not quantify the viscosity of the coating. This study is unique in this aspect. Polyethylene (PE) is used as a proxy for the organic material. A Dimer Coagulation, Isolation and Coalescence (DCIC) technique (Marsh et al., 2018; Rothfuss and Petters, 2016) is used to generate mixed particles composed of PE/PE and PE/AS dimer~~s~~ particles. Viscosity and CCN activity of pure PE particles is quantified. Dimer morphology is varied from agglomerate to core-shell morphology. Critical supersaturation for these mixed particles is measured as a function of dry particle volume, particle morphology, and organic volume fraction. Atmospheric implications of the experiments are discussed.

2 Methods

The basic methodology for dimer particle preparation has been presented in detail elsewhere (Marsh et al., 2018; Rothfuss and Petters, 2016). Briefly, two monodisperse particle populations of opposite charge are generated using differential mobility analyzers (DMAs) operated with positive and negative polarity power supplies. The streams are merged and particles are given time to coagulate. Coagulated dimer~~s~~ particles from particles carrying +1/–1 charge are charge neutral and transmit through an electrostatic filter. The terms “monomer particle” or monomer are used to refer to particles transmitted by a single DMA and the term “dimer particle” or dimer are used to refer coagulated particles. These particles are available for further manipulation and measurement.

Figure 1 summarizes the specific setup that was used in this study. Ammonium sulfate particles were generated using a constant output atomizer (TSI 3076) that was supplied with 0.1 % w/w AS solution using a syringe pump operated at 40 μL $\mathrm{min^{-1}}$ flow rate. The particles were dried using two Nafion dryers (Permapure PD-50T-24MSS) and charge neutralized using a ^{210}Po source. Monodisperse negatively-charged 50 nm AS particles were selected using the first DMA operated with sheath-to-sample flow ratios of 5 L $\mathrm{min^{-1}}$:1 L $\mathrm{min^{-1}}$ and connected to a positive polarity power supply (TSI-DMA1, TSI 3071). Monodisperse AS particles prepared in this way are nearly spherical with a dynamic shape factor of 1.02–1.06, depending on diameter and drying rate (Mikhailov et al., 2009; Zelenyuk et al., 2006).

Polyethylene particles were generated by homogeneous nucleation from vapor. A few beads of a PE standard (Restek, Polywax-850) were heated above its melting point (107 °C) in a round bottom, two-neck glass flask. Dry particle free N_2 boiled off from a Dewar was supplied trough the center neck. Nitrogen was used to prevent oxidation. A polydispersion of particles formed from homogenous nucleation and Brownian coagulation. Particles were size selected using a second DMA (TSI-DMA2, TSI 3071) also operated with sheath-to-sample flow ratios of 5 L $\mathrm{min^{-1}}$:1 L $\mathrm{min^{-1}}$ but using a negative voltage power supply to select positively charged particles. The polydisperse PE particles are likely glassy at room temperature (discussed further below) and heavily agglomerated. Therefore, the PE particles were passed through two sintering loops. The first sintering loop is after the initial cooling of the PE aerosol, the second after TSI-DMA2. Within the sintering loop the aerosol is heated to >90 °C, which lowers the viscosity sufficiently for the particles to relax into solid, near spherical particles.

The outflows from TSI-DMA1 and TSI-DMA2 were merged into three sequentially arranged 0.3 L capacity coagulation chambers (27 s average residence time). The flow was split after the chambers with 0.6 L min^{-1} being passed through an electrostatic filter to remove all charged particles. The charge neutral particles then passed through a temperature-controlled loop with residence time 5 s. The elevated temperature liquefied the PE such that dimer~~ized~~ particles changed from a dumbbell morphology into to a spherical morphology. ~~Since the melting point of AS (280 °C, Lide and Haynes, 2009) is much higher than that of PE (107 °C) the PE is expected to partially or fully engulf the AS core.~~ Particles exiting the conditioner were charge equilibrated using a ^{210}Po radiation source. The size distribution of coagulated particles was measured using a radial DMA (RDMA, Zhang et al., 1995) interfaced with a condensation nuclei (CN) counter (TSI 3020) and a streamwise thermal-gradient continuous flow CCN counter (Roberts and Nenes, 2005) as particle detectors. The CN and CCNc were operated at a total flow rate of 0.3 L min^{-1}, respectively. The CCNc and RDMA were operated using a sheath-to-sample flow ratio of 10:1 and 2 L min^{-1}:0.6 L min^{-1}, respectively. The RDMA was configured to measure the size distribution in scanning mobility particle sizer (SMPS) mode (Wang and Flagan, 1990), scanning voltage from 3000 to 100 V (145 – 26 nm) over 210 s. The coagulation chamber, electrostatic filter, and RDMA are housed inside a temperature-controlled box that can be varied between –20 °C to +40 °C. The temperature of the box is set to a baseline temperature where dimers do not relax into spherical shape and is referred to as the system temperature. Relative humidity at the system temperature was less than 3%, much drier than conditions where ammonium sulfate dimers were observed to relax into a spherical shape due to water uptake in Rothfuss and Petters (2016).

Since the melting point of AS (280 °C, Lide and Haynes, 2009) is much higher than that of PE (107 °C) the liquid PE is expected to partially or fully engulf the AS core. The assumed morphology of a liquid droplet on a spherical solid substrate depends on the solid/liquid, solid/vapor, liquid/vapor tensions, as well as the tension of the three phase contact line (Iwamatsu, 2016). The equilibrium morphology of this system can be (1) core-shell morphology (complete wetting), (2) core-shell morphology with uneven coating thickness (cap shaped droplet), (3) partially engulfed morphology (cap shaped droplet), or (4) dumbbell shaped morphology (complete drying). Parenthetical terms correspond to those used by Iwamatsu (2016). The line tension term becomes increasingly important at smaller scales. Line tension drives the system toward core-shell morphology. There is insufficient information about the AS/PE system at 95 °C to theoretically evaluate the equilibrium morphology. However, the liquid/vapor tension of polyethylene melts is 0.034 J m^{-2} (Dettre and Johnson, 1966; Owens and Wendt, 1969) and in principle a low liquid/vapor tension will favor the spreading of liquid on a high-energy surface. Reid et al. (2011) argue that core–shell morphologies are favored for a liquid phase surrounding a solid crystalline core. Freedman et al. (2010) show that ammonium sulfate particles coated with palmitic acid (produced through a coating oven), remain in core-shell structure. Palmitic acid and liquid PE both have low liquid/vapor interfacial tension. Palmitic acid and PE are both dominated by CH_2 functional groups and thus the solid/liquid tension and line tension terms for these two substances should be similar.

The particles are cooled down to system temperature after they relax into spherical shape in the temperature-controlled loop. Based on the above we argue that the final morphology is a core-shell structure. However, we cannot dismiss the possibility that particles assumed a partially engulfed morphology. That morphology may be either due to equilibrium shape or arise during the annealing of the particle. ~~Upon cooling the PE coating anneals.~~ Thus, w~~W~~hether the coating of annealed PE is of uniform thickness is unknown. Scanning Electron Microscopy with Energy Dispersive X-ray spectroscopy of PE/AS dimer particles~~s~~ with larger diameters was attempted. However, the analysis was inconclusive due to insufficient resolution resulting from poor conductivity of the prepared samples and necessary limits in maximum electron beam intensity to ensure that the PE did not melt.

2. Experiment Types

2.1.1 Viscosity Measurement

Viscosity of pure PE particles was measured as described in previous publications (Marsh et al., 2018; Rothfuss and Petters, 2016, 2017). For this experiment, PE/AS and PE/PE dimers are prepared by feeding AS or sintered PE particles to TSI-DMA1 and sintered PE particles to TSI-DMA2. The temperature inside the thermal conditioner is continuously scanned from 25 °C (system temperature) to 95 °C over a period of 284 min. The mode of the size distribution is monitored by the RDMA-CN/CCNc instruments. The analysis of the data follows the same steps described previously and only given in abridged form. First, the raw size distribution is fitted to a lognormal distribution function to find the peak diameter. Then, the particle geometry factor is determined (Rothfuss and Petters, 2016)

$$\xi = \frac{3}{D_{uc}/D_c - 1}\left(\frac{D_p}{D_c} + \frac{D_{uc}/D_c - 4}{3}\right) \qquad (1)$$

where ξ is the particle geometry factor, D_p is the SMPS peak diameter, D_{uc} the fully uncoalesced and D_c is the fully coalesced dimer diameter. The diameters D_{uc} and D_c are determined from scans near the system temperature and scans near 95 °C, respectively. Next, the fitted mode diameters are binned into 3 K intervals (Marsh et al., 2018) and the mean geometry factor is derived for each bin. These data are then fitted to a logistic curve

$$\xi = 1 + \frac{3}{1 + exp[-k(T - T_r)]} \qquad (2)$$

where k represents the steepness, T is the measured temperature of the conditioning loop, and T_r is the relaxation temperature representative of the midpoint of the logistic curve. The shape factor is converted to viscosity, η via a lookup table of modified Frenkel sintering theory (Pokluda et al., 1997; Rothfuss and Petters, 2016). Conditioner residence time, monomer diameter, and surface tension assumed in the conversion are t = 5 s, D_{mono} = 50 nm, and σ = 0.034 J m^{-2}, respectively. The assumed surface tension is based on measured values for polyethylene melts (Dettre and Johnson, 1966; Owens and Wendt, 1969). The inferred viscosity is only weakly dependent on the assumed surface tension value (Marsh et al., 2018; Rothfuss and Petters, 2016). Particle shape factors vary between $1 \le \xi \le 4$, which map to a narrow range of viscosity between 10^{-5} Pa s and 3×10^{-6} Pa s for the selected conditioner residence time, monomer diameter, and surface tension. The inferred temperature dependent viscosity over this range is fitted to a modified Vogel-Fulcher-Tammann (VFT) equation (Rothfuss and Petters, 2017).

$$log_{10}\eta = A + \frac{B}{T - T_0} \tag{3}$$

where A, B, and T_0 are coefficients obtained from a least-square fit. By convention (Debenedetti and Stillinger, 2001), the glass transition temperature, T_g, corresponds to $\eta = 10^{12}$ Pa s. It is obtained by extrapolation of the VFT equation. Similarly, the temperature of the transition where $\eta = 5\times10^{6}$ Pa s, T_c, is computed from equation (3). This value is computed to aid comparison of transition temperatures from similar measurements made with this experimental setup.

2.1.2 Pure Compound CCN Measurement

The CCN instrument was calibrated using size-resolved CCN measurements. Size-resolved measurements of pure PE were also obtained. Ammonium sulfate was used to calibrate the CCN instrument supersaturation, which is set by the streamwise thermal gradient. Gradients between 6 and 20 °C were used. Ammonium sulfate experiments were performed using the system described in Petters and Petters (2016). Dried, charge-neutralized particles are passed through a DMA (TSI 3080) operated with sheath-to-sample flow ratio of 9 L min^{-1}:1.3 L min^{-1}. Particle concentration is measured using a condensation particle counter (TSI 3771) and the CCN instrument. The instrument is operated in scanning particle sizer mode with voltage downscan from 10kV to 10V. Activation diameter was obtained by a fit to the data and mapped to supersaturation (SS) using water activity from the Extended Aerosol Inorganics Model (E-AIM, Clegg et al., 1998). The resulting relationship between SS and temperature gradient is shown in the Supporting Online information.

The CCN activity of sintered PE was measured using a similar setup. A high-flow DMA column (Stolzenburg et al., 1998) operated at 9:2 L min^{-1} flow ratio was used. The high-flow column was used to access larger particle diameters. The CCN instrument was operated at a gradient of 20 °C and a total flow rate of 1 L min^{-1} to maximize the instrument supersaturation. First, a calibration with AS particles was attempted but particles activated at all sizes. Another calibration material, glucose was used. Glucose was selected because it is relatively less CCN active than AS (Petters and Petters, 2016; Rosenørn et al., 2006), forms near spherical test particles (Suda and Petters, 2013), and water activity vs. composition is known from bulk data (Miyajima et al., 1983).

2.1.3 Morphology CCN Measurements

Morphology CCN experiments proceeded on dimers with the thermal conditioner at room temperature (dumbbell morphology) and the thermal conditioner at ~95 °C (spherical morphology). Experiments were performed for AS and PE monomers as well as PE/PE and PE/AS dimers with different volume fractions. The CCNc was operated ramping nominal temperature gradients from 7 to 16 °C (0.30 to 0.66% SS) in discrete steps. At each step 3 SMPS scans were performed. For PE/AS dimers with different volume fractions (shell thickness), 50 nm diameter AS monomers were coagulated with either 60 or 80 or 100 or 120 nm diameter PE monomers. These dimers were analyzed using the same method but limiting the nominal temperature gradients between 10 and 15 °C (0.42 to 0.62% SS).

The mobility diameter of the dimer depends on the particle morphology. From previous experiments with similar setups we found that the mobility diameters of uncoalesced dimers of equal size are between 1.04 and 1.1 times larger than the mobility dimeter of coalesced dimers (Marsh et al., 2018; Rothfuss and Petters, 2016, 2017). The dry particle masses are identical in the coalesced and uncoalesced states. Furthermore, as shown below, the PE itself is CCN inactive and does not contribute to the solute effect. Thus, the activation of PE/AS dimers is solely controlled by the AS monomer mass, which is unchanged in all experiments, and the kinetics of water transfer to the activating drop. The latter factor may differ with morphology and by extension mobility diameter. Therefore, the activated fraction was determined as follows. The monomer or dimer size and CCN response functions were fitted to a lognormal distribution function. The activated fraction (AF), i.e. the ratio of CCN to CN, was taken at the mode diameter of the size distribution. The activated fraction was then calculated for each scan at a particular supersaturation. A cumulative Gaussian distribution function (CDF) was used to fit the AF vs. SS relationship. The activation supersaturation SS_{50} corresponding to the SS at which AF equals to 0.5 was considered to be the critical supersaturation (Petters et al., 2009).

3 Results

3.1 Pure compound CCN experiments

Raw data for the pure compound CCN experiments are provided in the Supporting Online Information. For PE monomers no activation was observed at the largest diameter for which sufficient particle counts could be generated (741 nm) and thermal gradient in the CCN instrument (20 °C). The exact supersaturation corresponding to the thermal gradient is unknown because most of the reference glucose particles of the smallest selected particle size activated at this setting (23.4 nm). Taking glucose $\kappa=0.17$ based on CCN measurements (Petters and Petters, 2016), this implies that SS > 2.5%. The combination of SS = 2.5% and $D = 741$ nm corresponds to a state above the Kelvin condition where insoluble but wettable particles activate ($\kappa = 0$, Petters and Kreidenweis, 2007). Polyethylene is hydrophobic and has a contact angle with water between 79 and 111° (Boulange-Petermann et al., 2003; Dann, 1970; Gotoh et al., 2000; Owens and Wendt, 1969). The absence of measurable CCN activity under the selected conditions is consistent with nucleation theory that includes contact angle (Fletcher, 1962; Mahata and Alofs, 1975). The results show that in mixed particles that are composed of AS and PE, the PE will not contribute dissolved solute. Therefore, a 50 nm dry AS particle and 50 nm dry AS particle mixed with PE are expected to activate at the same critical supersaturation provided that the contribution of PE to the wet particle volume at the point of activation remains small.

3.2 Viscosity Experiments

Two experiments were performed; temperature induced relaxation of PE/PE dimers, and relaxation of PE/AS dimers. Results from the two experiments are graphed in Figure 2. The graphs are included to illustrate the data reduction procedure through Eqs. (2) and (3). Fitted parameters from these experiments are summarized in Table 1. The main conclusions from these experiments are as follows. At $T > 80$ °C, the shape of the particles no longer changes, and the particle is fully coalesced. At those temperatures $\eta < 10^5$ Pa s. Extrapolation of the VFT curve shows that at $T \sim 20$ °C the estimated viscosity for PE is 10^{12} Pa s, which corresponds to a highly viscous, potentially glassy state. This extrapolation method has been shown to predict T_g within ±10 °C for sucrose and citric acid (Marsh et al., 2018; Rothfuss and Petters, 2017). Estimated T_c and T_r values between the two experiments are within 4 °C, consistent with prior results that show that relaxation of a viscous liquid around a solid particle produces similar results than the merging of two liquefying spheres (Rothfuss and Petters, 2017). The precise morphology of the fully coalesced PE/AS dimer is unknown. The change in mobility diameter for the PE/PE and PE/AS experiments was 5.96 and 5.88 nm, respectively. For PE/PE particles, this is consistent with expected dynamic shape factors for rods and the final diameter of the coalesced particles is spherical. The similarity of the shift suggests that PE/AS particles are also spherical, with liquid PE coating the AS at high temperature. ~~Upon cooling the PE coating anneals. Whether the coating of annealed PE is of uniform thickness is unknown. Scanning Electron Microscopy with Energy Dispersive X-ray spectroscopy of PE/AS dimers with larger diameters was attempted. However, the analysis was inconclusive due to insufficient resolution resulting from poor conductivity of the prepared samples and necessary limits in maximum electron beam intensity to ensure that the PE did not melt.~~

3.3 Morphology CCN Experiments

Figure 3 shows a typical morphology CCN experiment. The curves correspond to the SMPS scan using the CN and CCN as detector. The left panels correspond to measurements with AS monomers. For this experiment, TSI-DMA2 and the electrostatic filter were turned off. Thus, the experiment corresponds to a tandem DMA experiment with a second neutralizer placed in line. The resulting size distribution is trimodal over the range shown. Theoretical analysis and experimental verification of the size distribution produced by this tandem DMA configuration is provided elsewhere (Petters, 2018; Wright et al., 2016)[1]. Briefly, the center peak is dominated by singly charged particles transmitted by TSI-DMA1, the peak to the right is dominated by doubly charged particles that have undergone charge re-equilibration and the peak to the left is dominated by singly-charged particles transmitted by TSI-DMA1 that have acquired two charges during the charge re-equilibration step. At dT = 16K (SS = 0.66%) the CCN and CN distributions agree, indicating that particles of all sizes activated. Conversely, at

---

[1] ~~Petters, M.D. (2018) *A language to simplify computation of differential mobility analyzer response functions* submitted to Aerosol Science & Technology. The manuscript is undergoing peer-review and can be accessed on the publically available github repository: https://github.com/mdpetters/DifferentialMobilityAnalyzers.jl.~~ Theoretical analysis of the relevant response functions reported in this work is provided in Notebook S8. Hygroscopicity Tandem DMA and Notebook S10. Dimer Coagulation and Isolation, which are supplements to ~~the~~ Petters (2018) ~~manuscript~~.

dT = 8K (SS = 0.34%) none of the nominal 50 nm AS monomers activated, while most of the larger particles did. At dT = 12K (SS = 0.50%) an appreciable fraction of the 50 nm AS monomers activated.

The middle panels in Figure 3 correspond to measurements with 50 nm PE/50 nm AS dimers in their uncoalesced state (dumbbell morphology). The measured size dimer distribution is also trimodal, although for reasons different than those of the tandem DMA experiment. The shape of the dimer size distribution has been analyzed elsewhere (Petters, 2018; Rothfuss and Petters, 2016). Briefly, the center peak is dominated by dimers formed from +1/–1charged particles transmitted by TSI-DMA1 and TSI-DMA2. The peak to the right is dominated by dimers formed from coagulated +2/–2 charged particles. The peak to the left is dominated by monomers that lost their charge on transit between either size-selection DMA and the electrostatic filter. Note that at the mode of the center peak, the solute volume of AS is identical to that of the monomer experiment shown in the left panel. Consequently, the center peak is used for analysis. The ratio of CN and CCN at the mode diameter of the center peak for dT = 8, 12, and 16K are very similar to that of the monomer experiment. The only difference between the middle panel and right panel in Figure 3 is the temperature of thermal conditioner. The center mode corresponding to the +1/–1 dimers is reduced by 4.4 nm (Table S8), indicating the change in particle morphoplogy while holding the number of AS and PE molecules comprising the particle constant. The dimers in their coalesced state represent the core/shell morphology. Assuming a uniform coverage, the thickness of the PE shell is 6.5 nm. Again, the ratio of CN and CCN at the mode diameter of center peak for dT = 8, 12, and 16K are very similar to that of the monomer experiment.

Figure 4 shows the relationship between AF and SS at the mode diameter for 50 nm AS monomers, uncoalesced 50 nm AS/50 nm PE dimers and fully coalesced 50 nm AS/50 nm PE dimers shown in Figure 3. Here the discrete supersaturation values correspond to steps in dT = 1K, i.e. dT = 8, 9, … , 16K (0.34 to 0.66% SS). The fitted activation spectra for the three experiments are virtually identical. Although there is some scatter in the AF data, the activation occurred at the same dT in all three cases. This implies that the CCN activation is controlled by only the AS core. Addition of hydrophobic PE to the particle has no effect, irrespective of particle morphology.

The experiment was repeated with 50 nm AS and 60, 80, 100 and 120 nm size PE dimers to vary the nominal coating thickness. These experiments are summarized in Figure 5. The volume fraction of PE varied from 50% to 96.7%, corresponding to nominal coating thickness between 6.5 and 36.4 nm. The dimer data were obtained in the coalesced state and the monomer data are shown for reference. Again, no significant differences in the activation supersaturation are observed. In some experiments, the activated fraction did not approach unity at high supersaturation. For experiments with disparate diameter of AS and PE, e.g. 50 nm AS and 120 nm PE, the dimer diameter will approach that of the larger monomer. Since a small fraction of decharged monomers also transmits (Rothfuss and Petters, 2016, Petters, 2018), the distribution contains some fraction of pure PE particles that will not activate. Thus, the lack of 100% activation at high SS is likely an artifact and not due to particle morphology. However, it is also possible that those particles are composed of PE/AS and have assumed a core-shell morphology that is sufficient to hinder activation.

4 Discussion

Question about how organic coatings influence CCN activity date back to Bigg (1986), who attributed poor aerosol-to-CCN closure to organic coatings. The two principle mechanisms of the delay are poor mass accommodation and diffusional limitation through the organic matrix (e.g. Chuang et al., 1997, Nenes et al., 2001, Zobrist et al., 2011). Either effect also implies some influence of particle morphology on CCN activation. Core-shell structures might be shielded by the organic while agglomerates or homogeneous mixtures are not.

Hygroscopic organic compounds that dissolve will not shield inorganic substances, even if they are initially glassy. Dissolution kinetics in crystalline substances occur on time scales faster than exposure time in CCN instruments (a few seconds) or cloud updrafts (few minutes) (Asa-Awuku and Nenes, 2007). This is corroborated by CCN experiments with sparingly soluble hygroscopic compounds that activate at their deliquescence RH, e.g. succinic or adipic acid. In their most pure state, these compounds activate according to theoretical prediction from solubility (Bilde and Svenningsson, 2004; Christensen and Petters, 2012; Hings et al., 2008; Hori et al., 2003; Kreidenweis et al., 2006), which implies no kinetic limitation to deliquescence and dissolution for crystalline solids at the time scale of CCN experiments. Amorphous glassy particles correspond to a less ordered state than crystalline solids. One might therefore expect a lower barrier to dissolution. Rothfuss et al. (2018) measured the condensation kinetics of water on amorphous glassy hygroscopic organic supermicron particles and found only marginal delays due to high starting viscosity. Extrapolation to submicron scales yields equilibration times ~100 ms, too fast to affect CCN experiments. The cited fundamental arguments are also consistent with the finding that water soluble and/or hygroscopic organic compounds have not shown growth delays or activation delays in coating studies (Cruz and Pandis, 2000; Garland et al., 2005; Hämeri et al., 1992). Based on this evidence, hygroscopic glassy organic substances can be ruled out to affect CCN activity through growth delays, irrespective of particle morphology.

Hydrophobic liquid organic substances may shield the inorganic core through mass accommodation effects. The studies discussed in the introduction (Abbatt et al., 2005; Nguyen et al., 2017; Xiong et al., 1998) suggest that thick coatings of lauric, stearic or palmitic acid are needed to achieve noticeable growth delays or deviation from ZSR mixing. The results by Nguyen et al. (2017) show a remarkable difference between saturated and unsaturated fatty acids, with saturated fatty acids hindering water transfer. It is known that the barrier efficiency increases with increasing organic chain length and packing density (McNeil et al., 2013). Packing density increases with attractive forces between molecules; the surface active fatty acids can bind on the hydrophobic tails and hydrophilic end groups. Lauric (C12) and palmitic (C16) acid are also macroscopic solids at room temperature due to their melting points of 44 and 63 °C, respectively (Lide and Haynes, 2009). These values are 63 and 44 °C cooler than that of the PE standard used here (107 °C). Assuming a similar shape of the VFT curve for fatty acids and PE, this implies that the viscosity of amorphous palmitic acid coatings at room temperature is $< 10^6$ Pa s. Some retardation based on viscosity is therefore expected for the fatty acids, although the viscosity is orders of magnitude lower than that of the glassy PE. The experiments here were motivated to generate core-shell structures that are both glassy and hydrophobic to investigate if the combination of the two effects will modify CCN activity. Before discussing possible reasons why no decline in CCN activity was observed, the nature of hydrophobic glassy particles is discussed.

Organic compounds become viscous and glassy due to the presence of functional groups. Rothfuss and Petters (2017) rank the sensitivity of viscosity to functional group addition from most to least sensitive as carboxylic acid (COOH) ≈ hydroxyl (OH) > nitrate (ONO_2) > carbonyl (CO) ≈ ester (COO) > methylene (CH_2). With the exception of nitrate groups, functional groups that are responsible for high viscosity also promote hygroscopicity (Petters et al., 2016; Suda et al., 2014). To our knowledge, multifunctional nitrated organic compounds are not prevalent or rare in the atmosphere. Therefore, the only source of hydrophobic-glassy-particles are high molecular weight weakly functionalized hydrocarbons. The PE source used here had a nominal molecular weight of 850 Da, corresponding to ~60 CH_2 groups. The carbon number may have changed during heating via thermal decomposition~~necessary for particle generation~~. Whether or not this occurred cannot be determined from the available data. Regardless, the obtained PE particles had an estimated viscosity of 10^{12} Pa s at room temperature. The exact carbon number of the PE particles here is not important, addition or subtraction of a few CH_2 molecules does not significantly alter viscosity or hygroscopity (Petters et al., 2016; Rothfuss and Petters, 2017). Note, however, that atmospherically relevant hydrophobic organics may have double bonds, include aromatic rings (e.g. polycyclic aromatic hydrocarbons), and may include some functional groups other than CH_x. Nonetheless, t~~T~~he PE particles used here are ~~therefore~~ used as a proxy for hydrophobic and glassy compounds. What then are plausible reasons that the PE model did not affect CCN activity?

The experiments in Figure 5 can be used to bound the water diffusivity. A nominal coating thickness of 36.4 nm corresponds to a particle composed of 96.7% organic material by volume. Scaling analysis implies that the apparent diffusivity of water through the shell is $D > \sim 10^{-16}$ m^2 s^{-1}, much larger than values calculated from the Stokes-Einstein relation. This estimate assumes a uniform coating. In practice, the uniformity of the coating is unknown. At 95 °C, the estimated viscosity of PE is $< 10^5$ Pa s (Figure 2). The resulting particles are spherical. If we imagine the system as effectively liquid, the surface tension forces will lead to a completely engulfed core with uniform coating. After exiting the conditioning loop, the coating anneals. It is plausible that small fissures form in the curved shell, which would reduce the packing density and allow water to penetrate. It is also plausible that the resulting coating is not of uniform thickness due to annealing forces resulting in the core to be pushed off center. In the extreme case a partially engulfed morphology may result, which has been documented to occur in particles with slow drying rates (Altaf and Freedman, 2017; Nandy and Dutcher, 2018). Another possibility is that the known breakdown of the Stokes-Einstein equation (Chenyakin et al., 2017; Price et al., 2014) is strong enough to result in diffusion rates through glassy PE that exceed the apparent $D > \sim 10^{-16}$ m^2 s^{-1}. Indeed the measured diffusivity of water through low density PE films is $\sim 10^{-14}$ m^2 s^{-1} (Wang et al., 2011). Thus, any of the mentioned effects, cracks, non-uniform coating thickness, or faster than expected diffusion, could have contributed to, or fully explain the lack of shielding observed in this study. Note that the saturated fatty acids for which delays have been observed have viscosity $< 10^6$ Pa s, which is low enough to allow viscous flow at the scale of submicron particles, and consequently the formation of a tightly packed viscous shell without cracks. This might suggest that the optimal barrier for shielding particles from water would be for substances that have a narrow range of viscosity where the coating is viscous enough to slow water transport but not too viscous to prevent flow around the particle.

These findings have important atmospheric implications. The permeability of polymers to small molecules is well known. For example, Nafion membrane humidifiers are widely used in the community for drying or humidifying aerosol flows (and are permeable to water vapor). Permeability depends on the polymer composition, its molecular weight, temperature, and the number and type of crosslinks (George and Thomas, 2001). A key question is what types of oligomeric or polymeric substances could form atmospheric hydrophobic glassy coatings, and by what process. Three are imagined here. Long-chain fatty acid coatings may form on sea-spray particles during the bubble-bursting process (Tervahattu, 2002). Some of these will initially be liquid and might turn glassy upon cooling or functionalization via heterogeneous aging. Weakly oxidized oils in the C_{18}-C_{40} range are emitted by diesel engines (Sakurai et al., 2003). These compounds may form coatings on pre-existing atmospheric particles perhaps through an evaporation-oxidation-condensation mechanism (Robinson et al., 2007) and also become glassy upon cooling or functionalization via heterogeneous aging. A third possibility is the irreversible oligomerization of weakly functionalized low molecular weight organic compounds forming hydrophobic compounds that then deposit on the surface of inorganic particles during drying (Altaf and Freedman, 2017; Nandy and Dutcher, 2018), followed by turning glassy during cooling. It is unclear how common and important these processes might be in the atmosphere. To our knowledge single particle studies on dried aerosol do not show core-shell structures as the dominant particle type (Laskin et al., 2012; Li et al., 2010; Piens et al., 2016). Regardless, the imagined processes producing hydrophobic glassy coatings undergo drying and cooling cycles that will be susceptible to the same ~~three~~ issues reported here: cracks, ~~and~~ non-uniform coating thickness formed during drying or annealing, partially engulfed equilibrium morphology, and faster than expected diffusion through hydrocarbon films. We therefore conclude that mass transfer limitation by glassy organic shells is unlikely to affect cloud droplet activation in the majority of cases at temperatures prevalent in the lower atmosphere. Extension of this result to temperatures in the upper free troposphere where low temperature slows diffusion may require further experimentation.

Altaf et al. (2018) report experiments that suggest that dry particle morphology impacts the activation diameter. These experiments were performed with particle mixtures composed of 50/50 w/w mixtures of AS/succinic and AS/pimelic acid particles. Particle morphology was varied by changing the drying rate; a slow drying rate produces particles with partially engulfed morphologies while a fast drying-rate produces particles with homogeneous morphology. The authors report that the partially engulfed morphologies activate at a smaller diameter than the homogeneous morphology. This result is opposite from the one reported here, where no effect of particle morphology on CCN activity was observed. The experiments here and by Altaf et al. (2018) differ in two key aspects. First, organic material between the two studies is different. Polyethylene is hydrophobic and does not contribute to the solute effect. Succinc and pimelic acid do. Succinc and pimelic acid also slightly lower surface tension of the air/aqueous solution interface, while PE does not. Second, the amount of solute is controlled differently in this study. Here, dimer morphology is produced by coagulation with fixed AS monomer size. In contrast, Altaf et al. (2018) used atomized mixtures, followed by drying and size selection. Altaf et al. (2018) do not have a quantitative theory to predict the observed effect of particle morphology but they propose potential explanations. One proposed explanation is that pimelic acid serves heterogeneous catalyst, the other proposed explanation is a liquid-liquid phase separation mechanism coupled with surface tension lowering similar to the mechanism proposed by (Ovadnevaite et al., 2017). Neither of these effects is applicable to the PE model system. However, we point out that the methodology used here can be used to create core-shell structures with many combinations of inorganic cores and organic coatings to further investigate effect of particle morphology on CCN activation for core-shell structures with organic shells that may lower surface tension.

5 Conclusions

Dimers composed of ammonium sulfate (AS) and polyethylene (PE) and PE and PE were prepared. The dimers were used to determine the temperature dependence of the viscosity of the generated PE particles by measuring the conditions where dimers coalesce and relax into spheres. The viscosity of PE was 5×10^{6} Pa s at 60 °C. Extrapolation of the temperature dependence suggests that the PE particles have viscosity 10^{12} Pa s near room temperature. Seven hundred nanometer diameter PE particles were CCN inactive at 2.5% supersaturation consistent with a contact angle of PE with water exceeding 79°. The AS/PE dimers were used to measure the critical supersaturation of the particles in dumbbell morphology formed during coagulation and core-shell morphology formed after shape relaxation. No difference in activation supersaturation was observed up to nominal shell thickness of 36.4 nm. An increase in supersaturation is expected if water diffusion was governed by the Stokes-Einstein relation. The apparent water diffusion through the hydrophobic plastic is orders of magnitude faster than predicted from the Stokes-Einstein relation. Potential explanations are cracks formed during annealing, non-uniform coating thickness, formation of partially engulfed morphologies, or fast diffusion of small molecules through polymer membranes. It is argued that processes that may form glassy hydrophobic organic shells on atmospheric particles will result in similar imperfect shielding of hygroscopic cores. However, particles with thick coatings of some, but not all fatty acids are an exception to the preceding claim (Abbatt et al., 2005, Nguyen et al., 2017, Forestieri et al., 2018). Water transfer will be less hindered in hydrophilic glassy organic materials due to the plasticizing effect of water on dissolving organic compounds. Based on literature data, particles comprising hydrophobic glassy organic materials fully coating inorganic cores are not ubiquitous in the atmosphere. Furthermore, timescales of humidification are shorter in CCN instruments than in atmospheric updrafts. Therefore, our experiments suggest that, near laboratory temperatures, mass transfer limitation by glassy organic shells is unlikely to affect cloud droplet activation.

6 Data availability

All data underlying the figures are available from the Online Supplement.

7 Supplement link (will be included by Copernicus)

8 Author contributions

MDP designed the experiments. AT and NE carried out the experiments. AT and MDP prepared the manuscript with contributions from all co-authors.

9 Competing interests

The authors declare that they have no conflict of interest.

10 Acknowledgements

This research was funded via Department of Energy, Office of Science grant DE-SC 0012043. AT acknowledges Central University of Himachal Pradesh for granting study leave to carry out this work at North Carolina State University.

11 References

Abbatt, J. P. D., Broekhuizen, K. and Pradeep Kumar, P.: Cloud condensation nucleus activity of internally mixed ammonium sulfate/organic acid aerosol particles, Atmos. Environ., 39, 4767–4778, doi:10.1016/j.atmosenv.2005.04.029, 2005.

Altaf, M. B. and Freedman, M. A.: Effect of Drying Rate on Aerosol Particle Morphology, J. Phys. Chem. Lett., 8(15), 3613–3618, doi:10.1021/acs.jpclett.7b01327, 2017.

Altaf, M. B., Dutcher, D. D., Raymond, T. M. and Freedman, M. A.: Effect of Particle Morphology on Cloud Condensation Nuclei Activity, ACS Earth Sp. Chem., 2(6), 634–639, doi:10.1021/acsearthspacechem.7b00146, 2018.

Asa-Awuku, A. and Nenes, A.: Effect of solute dissolution kinetics on cloud droplet formation: Extended Köhler theory, J. Geophys. Res., 112(D22), D22201, doi:10.1029/2005JD006934, 2007.

Berkemeier, T., Shiraiwa, M., Pöschl, U., and Koop, T.: Competition between water uptake and ice nucleation by glassy organic aerosol particles, Atmos. Chem. Phys., 14, 12513-12531, https://doi.org/10.5194/acp-14-12513-2014, 2014.

Bigg, E. K.: Discrepancy between observation and prediction of concentrations of cloud condensation nuclei, Atmos. Res., 20(1), 81–86, doi:10.1016/0169-8095(86)90010-4, 1986.

Bilde, M. and Svenningsson, B.: CCN activation of slightly soluble organics: the importance of small amounts of inorganic salt and particle phase, Tellus B, 56(B), 128–134, doi:10.1111/j.1600-0889.2004.00090.x, 2004.

Boulange-Petermann, L., Debacq, C., Poiret, P. and Cromieres, B.: Effect of the physical chemistry of polymeric coating surfaces on fouling and cleanability with particular reference to the food industry, in Contact Angle, We~~r~~ttability and Adhesion, vol. 3, edited by K. L. Mittal, pp. 501–519, VSP BV., 2003.

Cappa, C. D., Che, D. L., Kessler, S. H., Kroll, J. H. and Wilson, K. R.: Variations in organic aerosol optical and hygroscopic properties upon heterogeneous OH oxidation. Journal of Geophysical Research: Atmospheres, 116, D15204, 2011.

Chang, R. Y.-W., Slowik, J. G., Shantz, N. C., Vlasenko, A., Liggio, J., Sjostedt, S. J., Leaitch, W. R., and Abbatt, J. P. D.: The hygroscopicity parameter (κ) of ambient organic aerosol at a field site subject to biogenic and anthropogenic influences: relationship to degree of aerosol oxidation, Atmos. Chem. Phys., 10, 5047-5064, https://doi.org/10.5194/acp-10-5047-2010, 2010.

Chenyakin, Y., Ullmann, D. A., Evoy, E., Renbaum-Wolff, L., Kamal, S. and Bertram, A. K.: Diffusion coefficients of organic molecules in sucrose–water solutions and comparison with Stokes–Einstein predictions, Atmos. Chem. Phys., 17(3), 2423–2435, doi:10.5194/acp-17-2423-2017, 2017.

Christensen, S. I. and Petters, M. D.: The Role of Temperature in Cloud Droplet Activation, J. Phys. Chem. A, 116(39), 9706–9717, doi:10.1021/jp3064454, 2012.

Chuang, P. Y., Charlson, R. J. and Seinfeld, J. H.: Kinetic limitations on droplet formation in clouds, Nature, 390, 594, 1997.

Ciobanu, V. G., Marcolli, C., Krieger, U. K., Weers, U. and Peter, T.: Liquid-liquid phase separation in Mixed Organic/Inorganic Aerosol Particles, J. Phys. Chem. A, 113, 10966–10978, doi:10.1021/Jp905054d, 2009.

Clegg, S. L., Brimblecombe, P. and Wexler, A. S.: Thermodynamic Model of the System $H^{+} - NH_{4}^{+} - SO_{4}^{2-} - NO_{3}^{-} - H_{2}O$ at Tropospheric Temperatures, J. Phys. Chem. A, 102(12), 2137–2154, doi:10.1021/jp973042r, 1998.

Cruz, C. N. and Pandis, S. N.: The effect of organic coatings on the cloud condensation nuclei activation of inorganic atmospheric aerosol, J. Geophys. Res., 103123(20), 111–13, doi:10.1029/98JD00979, 1998.

Cruz, C. N. and Pandis, S. N.: Deliquescence and hygroscopic growth of mixed inorganic - Organic atmospheric aerosol, Environ. Sci. Technol., 34(20), 4313–4319, doi:10.1021/es9907109, 2000.

Dann, J.~~—.~~: Forces involved in the adhesive process, J. Colloid Interface Sci., 32(2), 321–331, doi:10.1016/0021-9797(70)90055-X, 1970.

Debenedetti, P. G. and Stillinger, F. H.: Supercooled liquids and the glass transition, Nature, 410(6825), 259–267, doi:10.1038/35065704, 2001.

Dettre, R. H. and Johnson, R. E.: Surface properties of polymers, J. Colloid Interface Sci., 21(4), 367–377, doi:10.1016/0095-8522(66)90003-1, 1966.

Fletcher, N. H.: The Physics of Rainclouds, 1st ed., Cambridge University Press, Cambridge., 1962.

Forestieri, S. D., Staudt, S. M., Kuborn, T. M., Faber, K., Ruehl, C. R., Bertram, T. H., and Cappa, C. D.: Establishing the impact of model surfactants on cloud condensation nuclei activity of sea spray aerosol mimics, Atmos. Chem. Phys., 18, 10985-11005, https://doi.org/10.5194/acp-18-10985-2018, 2018. ~~Forestieri, S. D., Staudt, S. M., Kuborn, T. M., Faber, K., Ruehl, C. R., Bertram, T. H. and Cappa, C. D.: Establishing the Impact of Model Surfactants on Cloud Condensation Nuclei Activity of Sea Spray Aerosols, Atmos. Chem. Phys. Discuss., (March), 1–44, doi:10.5194/acp-2018-207, 2018.~~

Freedman, M. A., Baustian, K. J., Wise, M. E. and Tolbert, M. A.: Characterizing the Morphology of Organic Aerosols at Ambient Temperature and Pressure, Analytical Chemistry, 82(19), 7965–7972, 2010.

Garland, R. M., Wise, M. E., Beaver, M. R., DeWitt, H. L., Aiken, A. C., Jimenez, J. L. and Tolbert, M. A.: Impact of palmitic acid coating on the water uptake and loss of ammonium sulfate particles, Atmos. Chem. Phys., 5(7), 1951–1961, doi:10.5194/acp-5-1951-2005, 2005.

George, S. C. and Thomas, S.: Transport phenomena through polymeric systems, Prog. Polym. Sci., 26(6), 985–1017, doi:10.1016/S0079-6700(00)00036-8, 2001.

Gorkowski, K., Donahue, N. M. and Sullivan, R. C.: Emulsified and Liquid–Liquid Phase-Separated States of α-Pinene Secondary Organic Aerosol Determined Using Aerosol Optical Tweezers, Environ. Sci. Technol., 51(21), 12154–12163, doi:10.1021/acs.est.7b03250, 2017.

Gotoh, K., Tao, J. and Tagawa, M.: Acid–base interaction in adhesion of polymer particles to silanized silica in water/n–ethanol mixtures, in Acid-Base Interactions: Relevance to Adhesion Science and Technology, edited by K. L. Mittal, pp. 539–550, VSP, Utrecht, The Netherlands., 2000.

Gunthe, S. S., King, S. M., Rose, D., Chen, Q., Roldin, P., Farmer, D. K., Jimenez, J. L., Artaxo, P., Andreae, M. O., Martin, S. T., and Pöschl, U.: Cloud condensation nuclei in pristine tropical rainforest air of Amazonia: size-resolved measurements and modeling of atmospheric aerosol composition and CCN activity, Atmos. Chem. Phys., 9, 7551-7575, https://doi.org/10.5194/acp-9-7551-2009, 2009.

Hämeri, K., Rood, M. and Hansson, H.-C.: Hygroscopic properties of a NaCl aerosol coated with organic compounds, J. Aerosol Sci., 23, S437–S440, doi:10.1016/0021-8502(92)90443-Y, 1992.

Hings, S. S., Wrobel, W. C., Cross, E. S., Worsnop, D. R., Davidovits, P. and Onasch, T. B.: CCN activation experiments with adipic acid: effect of particle phase and adipic acid coatings on soluble and insoluble particles, Atmos. Chem. Phys., 8(14), 3735–3748, doi:10.5194/acp-8-3735-2008, 2008.

Hori, M., Ohta, S., Murao, N. and Yamagata, S.: Activation capability of water soluble organic substances as CCN, J. Aerosol Sci., 34(4), 419–448, doi:10.1016/S0021-8502(02)00190-8, 2003.

Iwamatsu, M.: Line tension and morphology of a sessile droplet on a spherical substrate, Phys. Rev. E, 93, 052804, 2016.

Jacobson, M. C., Hansson, H.-C., Noone, K. J. and Charlson, R. J.: Organic atmospheric aerosols: Review and state of the science, Rev. Geophys., 38(2), 267–294, doi:10.1029/1998RG000045, 2000.

Jimenez, J. L., Canagaratna, M. R., Donahue, N. M., Prevot, A. S. H., Zhang, Q., Kroll, J. H., DeCarlo, P. F., Allan, J. D., Coe, H., Ng, N. L., Aiken, A. C., Docherty, K. S., Ulbrich, I. M., Grieshop, A. P., Robinson, A. L., Duplissy, J., Smith, J. D., Wilson, K. R., Lanz, V. A., Hueglin, C., Sun, Y. L., Tian, J., Laaksonen, A., Raatikainen, T., Rautiainen, J., Vaattovaara, P., Ehn, M., Kulmala, M., Tomlinson, J. M., Collins, D. R., Cubison, M. J., Dunlea, J., Huffman, J. A., Onasch, T. B., Alfarra, M. R., Williams, P. I., Bower, K., Kondo, Y., Schneider, J., Drewnick, F., Borrmann, S., Weimer, S., Demerjian, K., Salcedo, D., Cottrell, L., Griffin, R., Takami, A., Miyoshi, T., Hatakeyama, S., Shimono, A., Sun, J. Y., Zhang, Y. M., Dzepina, K., Kimmel, J. R., Sueper, D., Jayne, J. T., Herndon, S. C., Trimborn, A. M., Williams, L. R., Wood, E. C., Middlebrook, A. M., Kolb, C. E., Baltensperger, U. and Worsnop, D. R.: Evolution of Organic Aerosols in the Atmosphere, Science (80-.)., 326(5959), 1525–1529, doi:10.1126/science.1180353, 2009.

Krieger, U. K., Marcolli, C., Reid, J. P.: Exploring the Complexity of Aerosol Particle Properties and Processes using Single Particle Techniques, Chem. Soc. Rev., 41, 6631−6662, 2012.

Kreidenweis, S. M., Petters, M. D. and DeMott, P. J.: Deliquescence-controlled activation of organic aerosols, Geophys. Res. Lett., 33(6), L06801, doi:10.1029/2005GL024863, 2006.

Laskin, A., Moffet, R. C., Gilles, M. K., Fast, J. D., Zaveri, R. A., Wang, B., Nigge, P. and Shutthanandan, J.: Tropospheric chemistry of internally mixed sea salt and organic particles: Surprising reactivity of NaCl with weak organic acids, J. Geophys. Res. Atmos., 117(D15), D15302, doi:10.1029/2012JD017743, 2012.

Li, W. J., Shao, L. Y. and Buseck, P. R.: Haze types in Beijing and the influence of agricultural biomass burning, Atmos. Chem. Phys., 10(17), 8119–8130, doi:10.5194/acp-10-8119-2010, 2010.

Lide, D. R. and Haynes, W. M., Eds.: CRC Handbook of Chemistry and Physics, 90th ed., CRC Press, Boca Raton, FL., USA., 2009.

Mahata, P. C. and Alofs, D. J.: Insoluble Condensation Nuclei: The Effect of Contact Angle, Surface Roughness and Adsorption, J. Atmos. Sci., 32(1), 116–122, doi:10.1175/1520-0469(1975)032<0116:ICNTEO>2.0.CO;2, 1975.

Marsh, A., Petters, S. S., Rothfuss, N. E., Rovelli, G., Song, Y. C., Reid, J. P. and Petters, M. D.: Amorphous phase state diagrams and viscosity of ternary aqueous organic/organic and inorganic/organic mixtures, Phys. Chem. Chem. Phys., 20(22), 15086–15097, doi:10.1039/C8CP00760H, 2018.

Massoli, P., Lambe, A. T., Ahern, A. T., Williams, L. R., Ehn, M., Mikkilä, J., Canagaratna, M. R., Brune, W. H., Onasch, T. B., Jayne, J. T., Petäjä, T., Kulmala, M., Laaksonen, A., Kolb, C. E., Davidovits, P., and Worsnop, D. R.: Relationship between aerosol oxidation level and hygroscopic properties of laboratory generated secondary organic aerosol (SOA) particles, Geophys. Res. Lett., 37, L24801, https://doi.org/10.1029/2010GL045258, 2010.

Nakao, S.: Why would apparent κ linearly change with O/C? Assessing the role of volatility, solubility, and surface activity of organic aerosols. Aerosol Sci. Technol., 51, 1377-1388, 2017.

McNeill, V. F., Sareen, N. and Schwier, A. N.: Surface-Active Organics in Atmospheric Aerosols, in Atmospheric and Aerosol Chemistry, edited by V. F. McNeill and P. A. Ariya, pp. 201–259, Springer-Verlag Berlin Heidelberg., 2013.

Mei, F., Setyan, A., Zhang, Q., and Wang, J.: CCN activity of organic aerosols observed downwind of urban emissions during CARES, Atmos. Chem. Phys., 13, 12155-12169, https://doi.org/10.5194/acp-13-12155-2013, 2013.

Mikhailov, E., Vlasenko, S., Martin, S. T., Koop, T. and Pöschl, U.: Amorphous and crystalline aerosol particles interacting with water vapor: conceptual framework and experimental evidence for restructuring, phase transitions and kinetic limitations, Atmos. Chem. Phys., 9(24), 9491–9522, doi:10.5194/acp-9-9491-2009, 2009.

Miyajima, K., Sawada, M. and Nakagaki, M.: Studies on Aqueous Solutions of Saccharides. I. Activity Coefficients of Monosaccharides in Aqueous Solutions at 25 °C, Bull. Chem. Soc. Jpn., 56(6), 1620–1623, doi:10.1246/bcsj.56.1620, 1983.

Nandy, L. and Dutcher, C. S.: Phase Behavior of Ammonium Sulfate with Organic Acid Solutions in Aqueous Aerosol Mimics Using Microfluidic Traps, J. Phys. Chem. B, 122(13), 3480–3490, doi:10.1021/acs.jpcb.7b10655, 2018.

Nenes, A., Ghan, S., Abdul-Razzak, H., Chuang, P. Y. and Seinfeld, J. H.: Kinetic limitations on cloud droplet formation and impact on cloud albedo, Tellus B, 53(2), 133-149, 2001.

Nguyen, Q. T., Kjær, K. H., Kling, K. I., Boesen, T. and Bilde, M.: Impact of fatty acid coating on the CCN activity of sea salt particles, Tellus B Chem. Phys. Meteorol., 69(1), 1304064, doi:10.1080/16000889.2017.1304064, 2017.

O'Meara, S., Topping, D. O., and McFiggans, G.: The rate of equilibration of viscous aerosol particles, Atmos. Chem. Phys., 16, 5299-5313, https://doi.org/10.5194/acp-16-5299-2016, 2016.

Ovadnevaite, J., Zuend, A., Laaksonen, A., Sanchez, K. J., Roberts, G., Ceburnis, D., Decesari, S., Rinaldi, M., Hodas, N., Facchini, M. C., Seinfeld, J. H. and O' Dowd, C.: Surface tension prevails over solute effect in organic-influenced cloud droplet activation, Nature, 546(7660), 637–641, doi:10.1038/nature22806, 2017.

Owens, D. K. and Wendt, R. C.: Estimation of the surface free energy of polymers, J. Appl. Polym. Sci., 13(8), 1741–1747, doi:10.1002/app.1969.070130815, 1969.

Pajunoja, A., Lambe, A. T., Hakala, J., Rastak, N., Cummings, M. J., Brogan, J. F., Hao, L., Paramonov, M., Hong, J., Prisle, N. L., Malila, J., Romakkaniemi, S., Lehtinen, K. E. J., Laaksonen, A., Kulmala, M., Massoli, P., Onasch, T. B., Donahue, N. M., Riipinen, I., Davidovits, P., Worsnop, D. R., Petäjä, T., and Virtanen, A.: Adsorptive uptake of water by semisolid secondary organic aerosols, Geophys. Res. Lett., 42, 3063–3068,https://doi.org/10.1002/2015GL063142, 2015.

Petters, M. D. and Kreidenweis, S. M.: A single parameter representation of hygroscopic growth and cloud condensation nucleus activity, Atmos. Chem. Phys., 7(8), 1961–1971, doi:10.5194/acp-7-1961-2007, 2007.

Petters, M. D., Carrico, C. M., Kreidenweis, S. M., Prenni, A. J., DeMott, P. J., Collett, J. L. and Moosmüller, H.: Cloud condensation nucleation activity of biomass burning aerosol, J. Geophys. Res. Atmos., 114(22), 1–16, doi:10.1029/2009JD012353, 2009.

Petters, M. D., Kreidenweis, S. M. and Ziemann, P. J.: Prediction of cloud condensation nuclei activity for organic compounds using functional group contribution methods, Geosci. Model Dev., 9(1), 111–124, doi:10.5194/gmd-9-111-2016, 2016.

Petters, S. S. and Petters, M. D.: Surfactant effect on cloud condensation nuclei for two-component internally mixed aerosols, J. Geophys. Res. Atmos., 121, 1878–1895, doi:10.1002/2015JD024090~~.~~, 2016.

Petters, M. D.: A language to simplify computation of differential mobility analyzer response functions, A. Sci. & Technol., 52(12), 1437–1451, doi:10.1080/02786826.2018.1530724, 2018.

Petters, S. S., Kreidenweis, S. M., Grieshop, A. P., Ziemann, P. J., & Petters, M. D.: Temperature- and humidity-dependent phase states of secondary organic aerosols, Geophys. Res. Lett., 46, https://doi.org/10.1029/2018GL080563, 2019.

Piens, D. S., Kelly, S. T., Harder, T. H., Petters, M. D., O'Brien, R. E., Wang, B., Teske, K., Dowell, P., Laskin, A. and Gilles, M. K.: Measuring Mass-Based Hygroscopicity of Atmospheric Particles through in Situ Imaging, Environ. Sci. Technol., 50(10), 5172–5180, doi:10.1021/acs.est.6b00793, 2016.

Pokluda, O., Bellehumeur, C. T. and Machopoulos, J.: Modification of Frenkel ' s Model for Sintering, AIChE J., 43(12), 3253–3256, doi:10.1002/aic.690431213, 1997.

Pöschl, U., Martin, S. T., Sinha, B., Chen, Q., Gunthe, S. S., Huffman, J. A., Borrmann, S., Farmer, D. K., Garland, R. M., Helas, G., Jimenez, J. L., King, S. M., Manzi, A., Mikhailov, E., Pauliquevis, T., Petters, M. D., Prenni, A. J., Roldin, P., Rose, D., Schneider, J., Su, H., Zorn, S. R., Artaxo, P. and Andreae, M. O.: Rainforest Aerosols as Biogenic Nuclei of Clouds and Precipitation in the Amazon, Science (80-.)., 329(5998), 1513–1516, doi:10.1126/science.1191056, 2010.

Prenni, A. J., Petters, M. D., Kreidenweis, S. M., DeMott, P. J. and Ziemann, P. J.: Cloud droplet activation of secondary organic aerosol, J. Geophys. Res.,112, D10223, doi:10.1029/2006JD007963, 2007.

Prenni, A. J., DeMott, P. J. and Kreidenweis, S. M.: Water uptake of internally mixed particles containing ammonium sulfate and dicarboxylic acids, Atmos. Environ., 37(30), 4243–4251, doi:10.1016/S1352-2310(03)00559-4, 2003.

Price, H. C., Murray, B. J., Mattsson, J., O'Sullivan, D., Wilson, T. W., Baustian, K. J. and Benning, L. G.: Quantifying water diffusion in high-viscosity and glassy aqueous solutions using a raman isotope tracer method, Atmos. Chem. Phys., 14(8), 3817–3830, doi:10.5194/acp-14-3817-2014, 2014.

Reid, J. P., Dennis-Smither, B. J., Kwamena, N.-O. A., Miles, R. E. H., Hanford, K. L. and Homer, C. J.: The morphology of aerosol particles consisting of hydrophobic and hydrophilic phases: hydrocarbons, alcohols and fatty acids as the hydrophobic component, Phys. Chem. Chem. Phys., 13(34), 15559–15572, 2011.

Reid, J. P., Bertram, A. K., Topping, D. O., Laskin, A., Martin, S. T., Petters, M. D., Pope, F. D. and Rovelli, G.: The viscosity of atmospherically relevant organic particles, Nat. Commun., 9(1), 1–14, doi:10.1038/s41467-018-03027-z, 2018.

Roberts, G. C. and Nenes, A.: A continuous-flow streamwise thermal-gradient CCN chamber for atmospheric measurements, Aerosol Sci. Technol., 39(3), 206–221, doi:10.1080/027868290913988, 2005.

Robinson, A. L., Donahue, N. M., Shrivastava, M. K., Weitkamp, E. A., Sage, A. M., Grieshop, A. P., Lane, T. E., Pierce, J. R. and Pandis, S. N.: Rethinking Organic Aerosols: Semivolatile Emissions and Photochemical Aging, Science (80-.)., 315(5816), 1259–1262, doi:10.1126/science.1133061, 2007.

Rosenørn, T., Kiss, G. and Bilde, M.: Cloud droplet activation of saccharides and levoglucosan particles, Atmos. Environ., 40(10), 1794–1802, doi:10.1016/j.atmosenv.2005.11.024, 2006.

Rothfuss, N. E. and Petters, M. D.: Coalescence-based assessment of aerosol phase state using dimers prepared through a dual-differential mobility analyzer technique, Aerosol Sci. Technol., 50(12), 1294–1305, doi:10.1080/02786826.2016.1221050, 2016.

Rothfuss, N. E. and Petters, M. D.: Influence of Functional Groups on the Viscosity of Organic Aerosol, Environ. Sci. Technol., 51(1), 271–279, doi:10.1021/acs.est.6b04478, 2017.

Rothfuss, N. E., Marsh, A., Rovelli, G., Petters, M. D. and Reid, J. P.: Condensation Kinetics of Water on Amorphous Aerosol Particles, J. Phys. Chem. Lett., 9(13), 3708–3713, doi:10.1021/acs.jpclett.8b01365, 2018.

Ruehl, C. R. and Wilson, K. R.: Surface Organic Monolayers Control the Hygroscopic Growth of Submicrometer Particles at High Relative Humidity, J. Phys. Chem. A, 118(22), 3952–3966, doi:10.1021/jp502844g, 2014.

Sakurai, H., Tobias, H. J., Park, K., Zarling, D., Docherty, K. S., Kittelson, D. B., McMurry, P. H. and Ziemann, P. J.: On-line measurements of diesel nanoparticle composition and volatility, Atmos. Environ., 37(9–10), 1199–1210, doi:10.1016/S1352-2310(02)01017-8, 2003.

Stewart, D. J., Cai, C., Nayler, J., Preston, T. C., Reid, J. P., Krieger, U. K., Marcolli, C. and Zhang, Y. H.: Liquid–Liquid Phase Separation in Mixed Organic/Inorganic Single Aqueous Aerosol Droplets, J. Phys. Chemistry A, 119(18), 4177–4190, 2015.

Stolzenburg, M., Kreisberg, N. and Hering, S.: Atmospheric Size Distributions Measured by Differential Mobility Optical Particle Size Spectrometry, Aerosol Sci. Technol., 29(5), 402–418, doi:10.1080/02786829808965579, 1998.

Suda, S. R. and Petters, M. D.: Accurate Determination of Aerosol Activity Coefficients at Relative Humidities up to 99% Using the Hygroscopicity Tandem Differential Mobility Analyzer Technique, Aerosol Sci. Technol., 47(9), 991–1000, doi:10.1080/02786826.2013.807906, 2013.

Suda, S. R., Petters, M. D., Yeh, G. K., Strollo, C., Matsunaga, A., Faulhaber, A., Ziemann, P. J., Prenni, A. J., Carrico, C. M., Sullivan, R. C. and Kreidenweis, S. M.: Influence of Functional Groups on Organic Aerosol Cloud Condensation Nucleus

Activity, Environ. Sci. Technol., 48(17), 10182–10190, doi:10.1021/es502147y, 2014.

Tervahattu, H., Juhanoja, J., Kupiainen, K.: Identification of an organic coating on marine aerosol particles by TOF-SIMS, J. Geophys. Res., 107(D16), 4319, doi:10.1029/2001JD001403, 2002.

Wang, M., Wu, P., Sengupta, S. S., Chadhary, B. I., Cogen, J. M. and Li, B.: Investigation of Water Diffusion in Low-Density Polyethylene by Attenuated Total Reflectance Fourier Transform Infrared Spectroscopy and Two-Dimensional Correlation Analysis, Ind. Eng. Chem. Res., 50(10), 6447–6454, doi:10.1021/ie102221a, 2011.

Wang, S. C. and Flagan, R. C.: Scanning Electrical Mobility Spectrometer, Aerosol Sci. Technol., 13(2), 230–240, doi:10.1080/02786829008959441, 1990.

Wright, T. P., Song, C., Sears, S. and Petters, M. D.: Thermodynamic and kinetic behavior of glycerol aerosol, Aerosol Sci. Technol., 50(12), 1385–1396, doi:10.1080/02786826.2016.1245405, 2016.

Xiong, J. Q., Zhong, M., Fang, C., Chen, L. C. and Lippmann, M.: Influence of Organic Films on the Hygroscopicity of Ultrafine Sulfuric Acid Aerosol, Environ. Sci. Technol., 32(22), 3536–3541, doi:10.1021/es980019q, 1998.

Zelenyuk, A., Cai, Y. and Imre, D.: From Agglomerates of Spheres to Irregularly Shaped Particles: Determination of Dynamic Shape Factors from Measurements of Mobility and Vacuum Aerodynamic Diameters, Aerosol Sci. Technol., 40(3), 197–217, doi:10.1080/02786820500529406, 2006.

Zhang, S.-H., Akutsu, Y., Russell, L. M., Flagan, R. C. and Seinfeld, J. H.: Radial Differential Mobility Analyzer, Aerosol Sci. Technol., 23(3), 357–372, doi:10.1080/02786829508965320, 1995.

Zobrist, B., Soonsin, V., Luo, B. P., Krieger, U. K., Marcolli, C., Peter, T. and Koop, T.: Ultra-slow water diffusion in aqueous sucrose glasses, Phys. Chem. Chem. Phys., 13(8), 3514–3526, 2011.

Table 1: Tabulated values for viscosity experiments. Symbols not defined above: ΔT is the 95% confidence interval of T_r determined from the fit, and RH is the relative humidity inside the coagulation chamber.

			Equation 2				Equation 3		
System	T_c [°C]	T_g [°C]	T_r [°C]	k [-]	ΔT [°C]	RH [%]	A [-]	B [-]	T_0 [K]
PE/AS	64.5	23.9	67.7	0.19	3.8	2.9	0.7	519	251
PE/PE	60.2	20.7	63.4	0.19	2.8	2.3	1.08	456	252

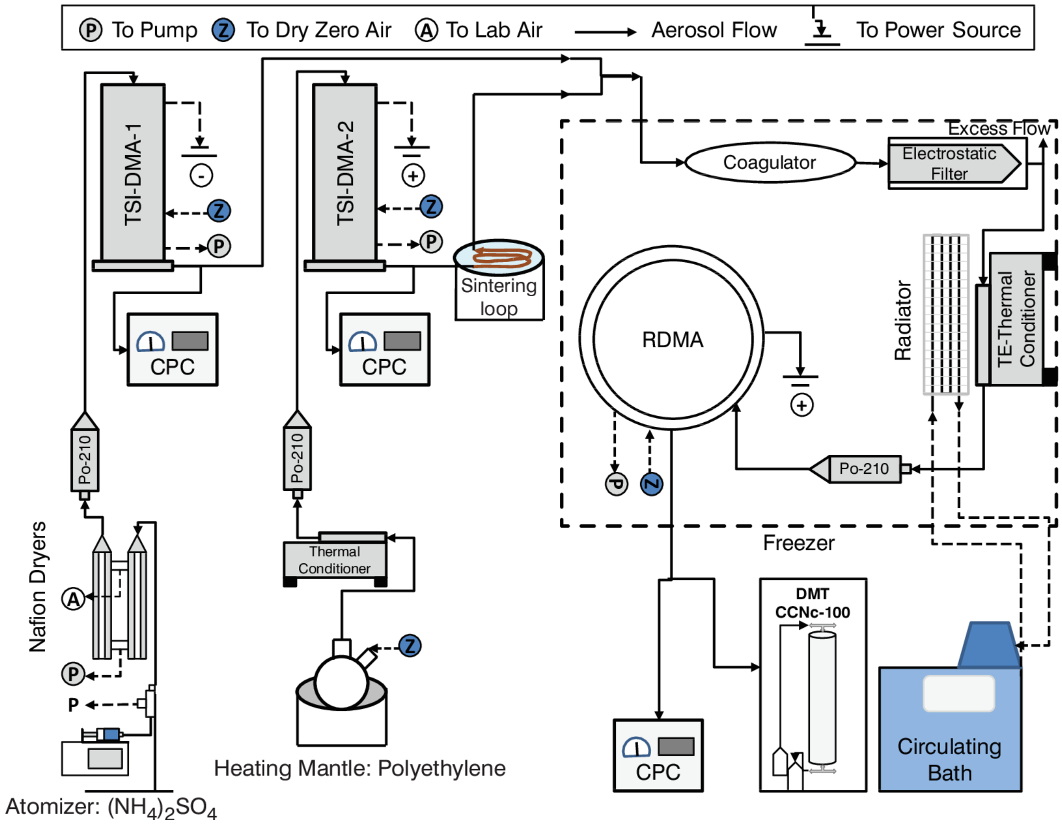

Figure 1: Schematic of the Experimental setup (DMA: Differential Mobility Analyzer, RDMA: Radial Differential Mobility Analyzer, CPC: Condensation Particle Counter, DMT CCNc-100: Cloud Condensation Nuclei Counter, Po-210: Polonium 210 radiation source).

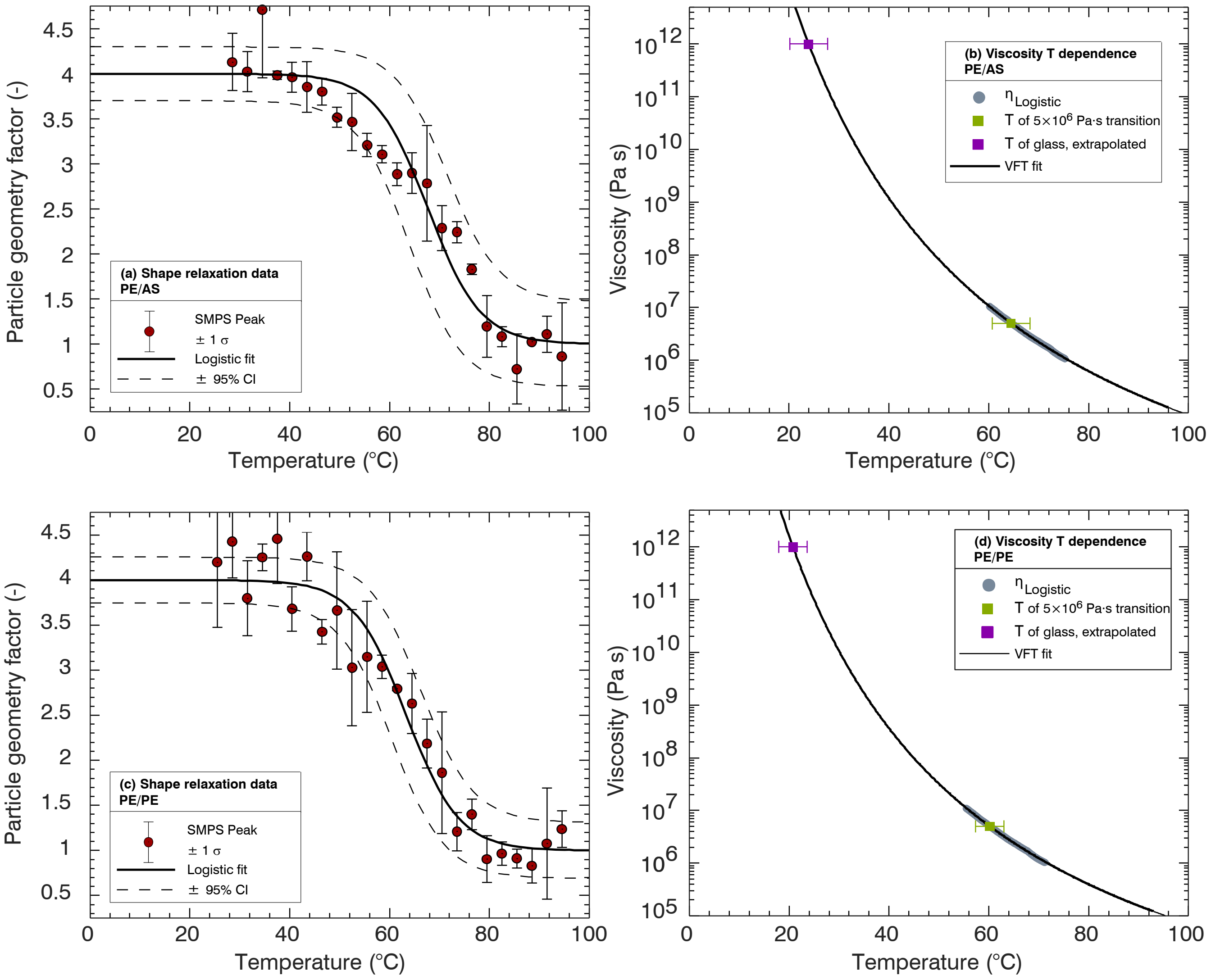

Figure 2. Left plots: shape relaxation data for PE/AS (a) and PE/PE (c) 50nm/50nm dimers. Symbols are the mean ~~shape~~ geometry factor derived from the temperature binned mode diameter peaks. Vertical bars are the standard deviation. Dashed lines correspond to the 95% confidence interval of the relaxation temperature derived from the fit. Right plots: ~~inferred viscosity~~ temperature dependence of viscosity for PE/AS (b) and PE/PE (d) experiments. The solid line gives the VFT fit. Grey circles correspond to values where $1 > \xi > 4$. The green and purple symbols correspond $\eta = 5\times10^6$ and 10^{12} Pa s, respectively. Horizontal error bars correspond to the 95% confidence interval of the relaxation temperature derived from the fit. Parameters corresponding to the logistic and VFT fits are given in Table 1.

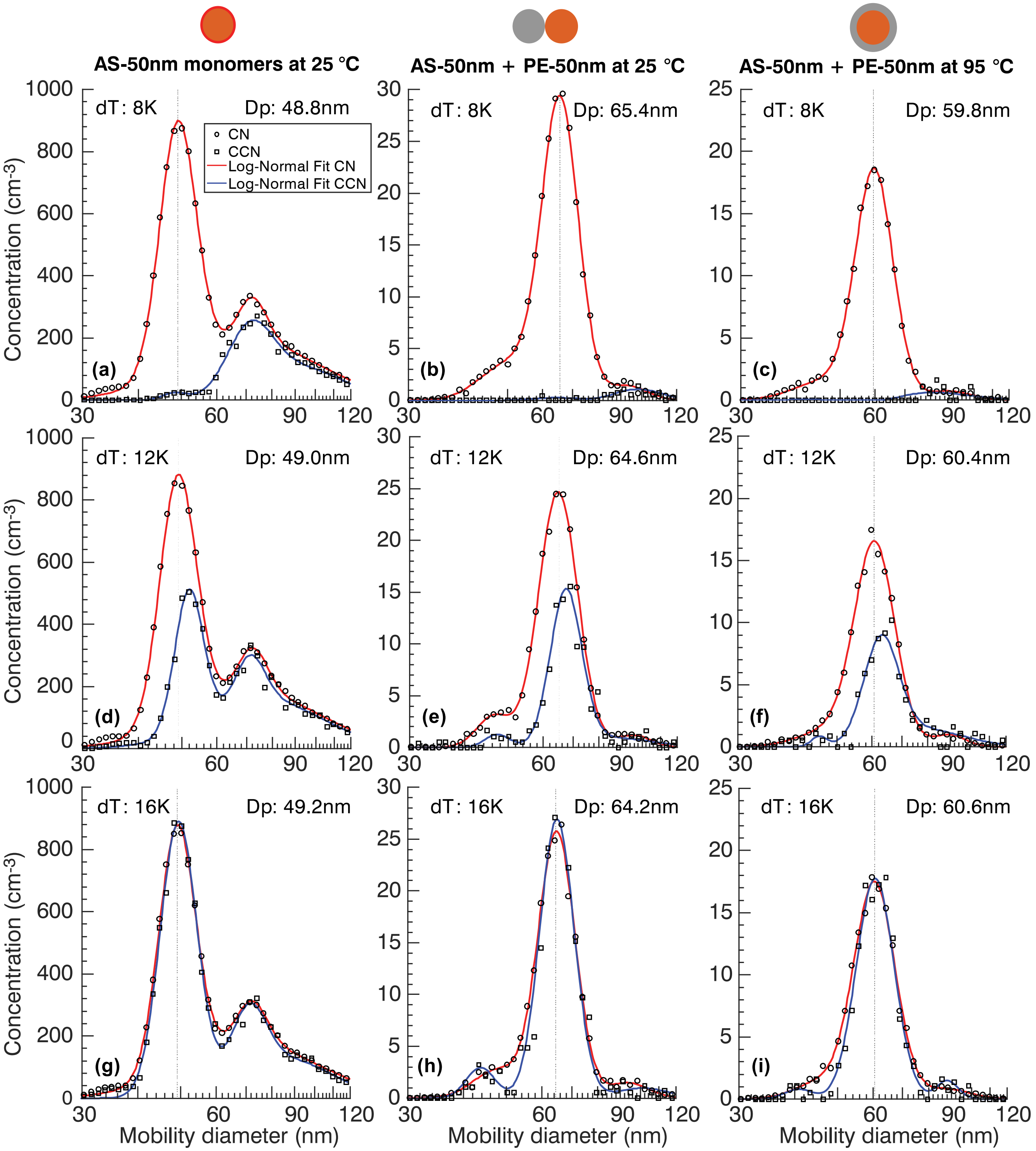

Figure 3: CN and CCN size-distributions at three different CCNc column temperature gradients corresponding to water supersaturations measured after the thermal conditioning of particles.

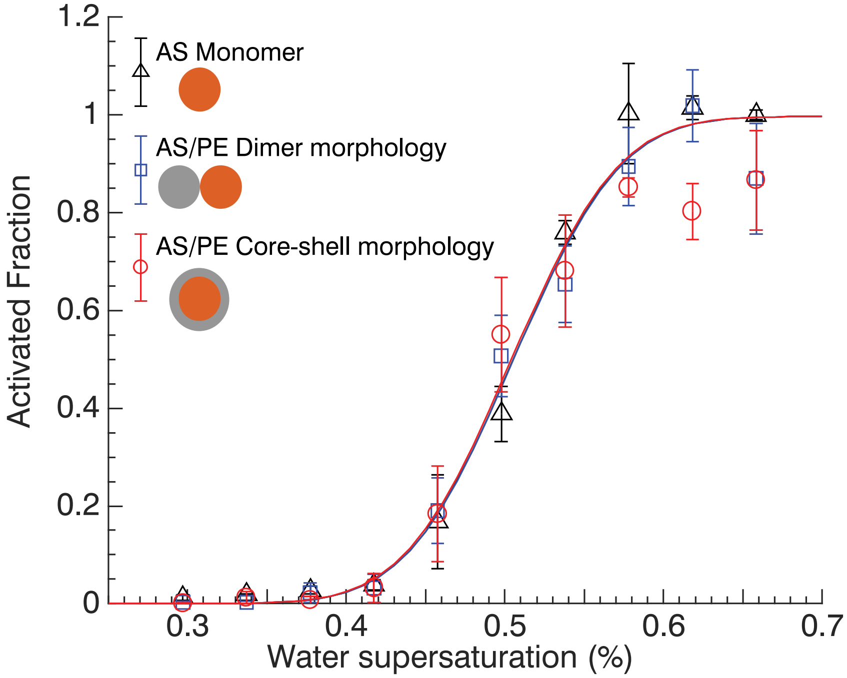

Figure 4: Activated fraction determined at mode diameter of ammonium sulfate monomers and mixed ammonium sulfate/polyethylene particles with dumbbell and core-shell morphology at different water supersaturation. Lines correspond to a fit to the data.

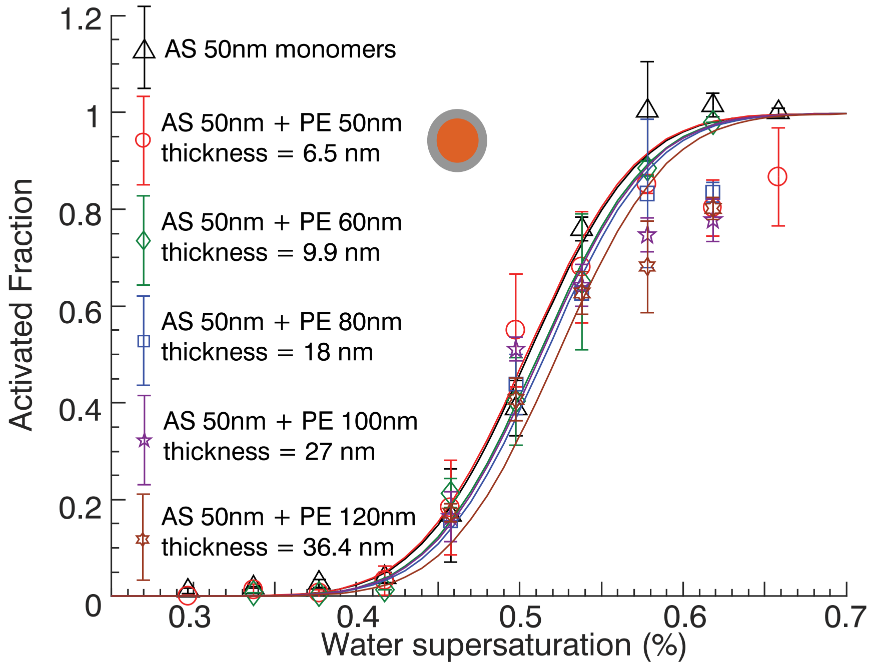

Figure 5: Activation properties of ammonium sulfate monomers and mixed ammonium sulfate/polyethylene particles with core-shell morphology with varying coating thickness. Error bars correspond to ±1 standard deviation associated with activated faction estimated from three separate scans.